

Permutation p -value approximation via generalized Stolarsky invariance

Hera Y. He, Kinjal Basu, Qingyuan Zhao, Art B. Owen

*Department of Statistics
Sequoia Hall
Stanford University
Stanford, CA 94305*

e-mail: ([yhe1](mailto:yhe1@stanford.edu), [kinjal](mailto:kinjal@stanford.edu), [qyzhao](mailto:qyzhao@stanford.edu), [owen](mailto:owen@stanford.edu))@stanford.edu

Abstract: It is common for genomic data analysis to use p -values from a large number of permutation tests. The multiplicity of tests may require very tiny p -values in order to reject any null hypotheses and the common practice of using randomly sampled permutations then becomes very expensive. We propose an inexpensive approximation to p -values for two sample linear test statistics, derived from Stolarsky's invariance principle. The method creates a geometrically derived set of approximate p -values for each hypothesis. The average of that set is used as a point estimate \hat{p} and our generalization of the invariance principle allows us to compute the variance of the p -values in that set. We find that in cases where the point estimate is small the variance is a modest multiple of the square of the point estimate, yielding a relative error property similar to that of saddlepoint approximations. On a Parkinson's disease data set, the new approximation is faster and more accurate than the saddlepoint approximation. We also obtain a simple probabilistic explanation of Stolarsky's invariance principle.

1. Introduction

Permutation methods are commonly used to obtain p -values in genomic applications. They make only modest assumptions and they have a direct intuitive interpretation that appeals to biologists in collaborations. In even modestly large data sets, the exact permutation p -value becomes too expensive to compute. Then Monte Carlo sampling of random permutations becomes a standard approach. Genomic applications commonly require thousands or more of hypotheses to be tested, and then multiplicity adjustment requires that some small p -values be obtained if any null hypotheses are to be rejected. When p -values below ϵ are required to reject H_0 , then [Knijnenburg et al. \(2009\)](#) recommend doing at least $10/\epsilon$ random permutations. As a result, even Monte Carlo sampling for permutation tests can be prohibitively expensive, and hence it pays to search for fast approximations to the permutation p -value.

In this paper we develop rapidly computable approximations to some permutation p -values. The p -values we consider are for a difference in group means. The approximations are based on ideas from spherical geometry and discrepancy, related to the Stolarsky invariance principle ([Stolarsky, 1973](#)). As described below, the resulting approximations prove to be very accurate for the tiny p -values where permutation methods are most difficult to use.

We begin with some background on the genomic motivation of our work. Then we transition to spherical geometry.

Genomic context

The specific problem that motivated us is testing for sets of genes associated with Parkinson’s disease (Larson and Owen, 2015). More details about this work are given in the the first author’s dissertation (He, 2016).

In these data sets, there are m_0 subjects without Parkinson’s disease and m_1 subjects with it. One can test whether Parkinson’s disease is associated with an individual gene by doing a t -test comparing gene expression levels in tissue samples from the two groups of subjects. Biological interest is often summarized more by gene sets rather than individual genes. Gene sets have two advantages: small but consistent associations of many genes with the test condition can raise power, and, the gene sets themselves often connect better to biological understanding than do individual genes. The null hypothesis is that the subject condition does not affect expression levels of any gene in the gene set.

There is a very large literature on testing for significant associations between a condition and the genes in a gene set. See Ackermann and Strimmer (2009) for an overview of the main concepts and methods in that literature. They did an extensive comparison of 261 different gene set testing methods and identified two families of winning methods. Let t_g be the ordinary two sample t statistic for comparing the average expression level of gene g between two conditions and let G be a set of genes of interest. They found that linear and quadratic test statistics $L_G = \sum_{g \in G} t_g$ and $Q_G = \sum_{g \in G} t_g^2$ had the best power, along with some simple approximations to those two statistics. These methods performed better than some substantially more complicated proposals. The statistic L_G was proposed by Jiang and Gentleman (2007). The statistic L_G and similar ones did best when expression differences between the two conditions tend to have the same sign, for each $g \in G$. If large but oppositely signed treatment effects occur, then Q_G and approximations to it do best.

The genes in a gene set are ordinarily correlated with each other, even if they are independent of the treatment condition. The correlations makes it difficult to find the null distributions of L_G and Q_G , even with parametric model assumptions. In a permutation analysis, like Ackermann and Strimmer (2009) use, we consider all $N = \binom{n}{m_1}$ different ways to select a subset π containing m_1 of the $n = m_0 + m_1$ subjects. Let Q_G^π be the test statistic recomputed as if those m_1 subjects had been the affected group. Then the permutation p -value for Q_G is

$$p = p_G = \frac{1}{N} \sum_{\pi} \mathbf{1}_{Q_G^\pi \geq Q_G}.$$

Note that the smallest possible value for p is $1/N$.

When N is too large for a permutation test to be computationally feasible, a standard practice is to estimate p via randomly sampled permutations of the treatment label as proposed by Barnard (1963). For $\ell = 1, \dots, M - 1$ we let

$\pi(\ell)$ be the affected group after a randomization of the treatment labels. We let $\pi(0)$ be the original allocation. Then the Monte Carlo estimate

$$\hat{p} = \frac{1}{M} \sum_{\ell=0}^{M-1} \mathbf{1}_{Q_G^{\pi(\ell)} \geq Q_G}$$

is used as an estimate of p , for the quadratic statistic. In this Monte Carlo, the true permutation p -value p is the unknown parameter and \hat{p} is the sample estimate of p . Note that $\hat{p} \geq 1/M$ because we have included the original allocation in the numerator. Failure to include the original allocation $\pi(0)$ can lead to $\hat{p} = 0$ which is very undesirable. We call $1/M$ the granularity limit. When p is quite small, an enormous number M of simulations may be required to get an accurate estimate of it. For instance, in genome wide association studies (GWAS) the customary threshold for significance is $\epsilon = 5 \times 10^{-8}$, making permutation methods prohibitively expensive, or even infeasible. For a recent discussion of p -value thresholds in GWAS, see [Fadista et al. \(2016\)](#).

In this paper, we work with one of Ackermann and Strimmer's (2009) approximations to L_G . Let $X_i = 1$ if subject i is in condition 1 and $X_i = 0$ for condition 0. Let Y_{ig} be the expression level of gene g for subject i . Let $\hat{\rho}_g$ be the sample correlation between X_i and Y_{ig} . Then $t_g = \sqrt{n - 2}\hat{\rho}_g / \sqrt{1 - \hat{\rho}_g^2}$ and a first order Taylor approximation gives $t_g \doteq \sqrt{n - 2}(\hat{\rho}_g + \hat{\rho}_g^3/2)$. When many small correlations $\hat{\rho}_g$ contribute to the signal, then summing $\hat{\rho}_g$ gives a test statistic that is almost equivalent to summing t_g . [Ackermann and Strimmer \(2009\)](#) found that

$$\sum_{g \in G} \frac{1}{n} \sum_{i=1}^n \frac{X_i - \bar{X}}{s_X} \frac{Y_{gi} - \bar{Y}_g}{s_g} \quad (1.1)$$

was in the same winning set of methods as L_G , where s_X and s_g are standard deviations of X_i and Y_{gi} respectively. They also considered using pooled variance estimates in place of s_g but found no advantage to doing so, perhaps because $\min(m_0, m_1)$ was at least 10 in their simulations. Letting $Y_i = Y_{Gi} \equiv \sum_{g \in G} Y_{gi}/s_g$, we may rewrite (1.1) as

$$\sum_{i=1}^n \frac{X_i - \bar{X}}{\|X - 1_n \bar{X}\|} \frac{Y_i - \bar{Y}}{\|Y - 1_n \bar{Y}\|} \quad (1.2)$$

multiplied by a constant that only depends on n and hence does not affect p . Equation (1.2) describes a test statistic that is a plain Euclidean inner product of two unit vectors in \mathbb{R}^n . Here \mathbf{x}_0 has i 'th component $(X_i - \bar{X})/\|X - 1_n \bar{X}\|$ and \mathbf{y}_0 is similar.

There are $N = \binom{n}{m_1}$ distinct vectors found by permuting the entries in \mathbf{x} . We label them $\mathbf{x}_0, \mathbf{x}_1, \dots, \mathbf{x}_{N-1}$ with \mathbf{x}_0 being the original one. Letting $\hat{\rho} = \mathbf{x}_0^\top \mathbf{y}_0$ we find that one and two-sided p -values for a linear statistic are

$$\frac{1}{N} \sum_{k=0}^{N-1} \mathbf{1}_{\mathbf{x}_k^\top \mathbf{y}_0 \geq \hat{\rho}} \quad \text{and} \quad \frac{1}{N} \sum_{k=0}^{N-1} \mathbf{1}_{|\mathbf{x}_k^\top \mathbf{y}_0| \geq |\hat{\rho}|}$$

repectively. We prefer two-sided test statistics, but we will study one-sided ones first and then translate our results to two-sided ones.

Spherical geometry

We are now ready to make a geometric interpretation. Let $\mathbb{S}^d = \{\mathbf{z} \in \mathbb{R}^{d+1} \mid \mathbf{z}^\top \mathbf{z} = 1\}$ be the d -dimensional unit sphere. Our data $\mathbf{x}_0, \mathbf{y}_0$ are in a subset of \mathbb{S}^{n-1} orthogonal to $\mathbf{1}_n$. That subset is isomorphic to \mathbb{S}^{n-2} and so we work mostly with $d = n - 2$.

Given a point $\mathbf{y} \in \mathbb{S}^d$, the points \mathbf{z} that are closest to \mathbf{y} comprise a spherical cap. The spherical cap of center \mathbf{y} and height $t \in [-1, 1]$ is $C(\mathbf{y}; t) = \{\mathbf{z} \in \mathbb{S}^d \mid \langle \mathbf{y}, \mathbf{z} \rangle \geq t\}$. By symmetry, $\mathbf{z} \in C(\mathbf{y}; t)$ if and only if $\mathbf{y} \in C(\mathbf{z}; t)$. The one-sided linear p -value is the fraction of \mathbf{x}_k for $0 \leq k < N$ that belong to $C(\mathbf{y}_0; \hat{\rho})$. A natural, but crude approximation to p is then

$$\hat{p}_1(\hat{\rho}), \quad \text{where} \quad \hat{p}_1(t) \equiv \frac{\text{vol}(C(\mathbf{y}_0; t))}{\text{vol}(\mathbb{S}^d)}.$$

Stolarsky's invariance principal gives a remarkable description of the accuracy of this approximation \hat{p}_1 . The squared L_2 spherical cap discrepancy of points $\mathbf{x}_0, \mathbf{x}_1, \dots, \mathbf{x}_{N-1} \in \mathbb{S}^d$ is

$$L_2(\mathbf{x}_0, \dots, \mathbf{x}_{N-1})^2 = \int_{-1}^1 \int_{\mathbb{S}^d} |\hat{p}_1(t) - p(\mathbf{z}, t)|^2 d\sigma_d(\mathbf{z}) dt$$

where $p(\mathbf{z}, t) = (1/N) \sum_{k=0}^{N-1} \mathbf{1}_{\mathbf{x}_k \in C(\mathbf{z}, t)}$ and σ_d is the uniform (Haar) measure on \mathbb{S}^d . [Stolarsky \(1973\)](#) shows that

$$\frac{d\omega_d}{\omega_{d+1}} \times L_2(\cdot)^2 = \int_{\mathbb{S}^d} \int_{\mathbb{S}^d} \|\mathbf{x} - \mathbf{y}\| d\sigma_d(\mathbf{x}) d\sigma_d(\mathbf{y}) - \frac{1}{N^2} \sum_{k,l=0}^{N-1} \|\mathbf{x}_k - \mathbf{x}_l\| \quad (1.3)$$

where ω_d is the (surface) volume of \mathbb{S}^d . Equation (1.3) relates the mean squared error of \hat{p}_1 to the mean absolute Euclidean distance among the N points. In our applications, the N points will be the distinct permuted values of \mathbf{x}_0 , but (1.3) holds for an arbitrary set of N points \mathbf{x}_k .

The left side of (1.3) is, up to normalization, a mean squared discrepancy over spherical caps. This average of $(\hat{p}_1 - p)^2$ includes p -values of all sizes between 0 and 1. It is not then a very good accuracy measure when $\hat{p}_1(\hat{\rho})$ turns out to be very small, such as 10^{-6} . It would be more useful to get such a mean squared error taken over caps of exactly the size $\hat{p}_1(\hat{\rho})$, and no others.

[Brauchart and Dick \(2013\)](#) consider quasi-Monte Carlo (QMC) sampling in the sphere. They generalize Stolarsky's discrepancy formula to include a weighting function on the height t . By specializing their formula, we get an expression for the mean of $(\hat{p}_1 - p)^2$ over spherical caps of any fixed size.

Discrepancy theory plays a prominent role in QMC ([Niederreiter, 1992](#)), which is about approximating an integral by a sample average. The present

setting is a reversal of QMC: the discrete average p over permutations is the exact value we seek, and the integral over a continuum is the approximation \hat{p} . A second difference is that the QMC literature focusses on choosing N points to minimize a criterion such as (1.3), whereas here the N points are determined by the problem.

As we will show below, the estimate \hat{p}_1 is the average of p over all spherical caps $C(\mathbf{y}; \hat{\rho})$ under a uniform distribution, i.e., $\mathbf{y} \sim \mathbf{U}(\mathbb{S}^d)$. Those caps have the same volume as $C(\mathbf{y}_0; \hat{\rho})$.

In addition to specializing from caps $C(\mathbf{y}; t)$ with $t = \hat{\rho}$ we can also specialize to caps whose centers \mathbf{y} more closely resemble \mathbf{y}_0 . Suppose that

$$\mathbf{y}_0 \in \mathbb{Y} \subset \mathbb{S}^d.$$

Then we know that $p(\mathbf{y}_0, \hat{\rho}) \leq \sup_{\mathbf{y} \in \mathbb{Y}} p(\mathbf{y}, \hat{\rho})$, which is a conservative permutation p -value. We are generally unable to compute this quantity but in some instances we can form a reference distribution $\mathbf{y} \sim \mathbf{U}(\mathbb{Y})$ and compute both $\mathbb{E}(p(\mathbf{y}, \hat{\rho}) \mid \mathbf{y} \in \mathbb{Y})$ and $\text{Var}(p(\mathbf{y}, \hat{\rho}) \mid \mathbf{y} \in \mathbb{Y})$, the mean and variance of $p(\mathbf{y}, \hat{\rho})$ under this distribution.

The simplest reference distribution we use has $\mathbb{Y}_1 = \mathbb{S}^d$. We have found that the set $\mathbb{Y}_2 = \{\mathbf{y} \in \mathbb{S}^d \mid \mathbf{y}^\top \mathbf{x}_0 = \mathbf{y}_0^\top \mathbf{x}_0\}$ and some generalizations yield especially useful reference distributions. Generalizations of the Stolarsky formula allow us to compute $\text{Var}(p(\mathbf{y}, \hat{\rho}) \mid \mathbf{y} \in \mathbb{Y}_2)$. In some of our numerical results from Section 7, we find that $\text{Var}(p(\mathbf{y}, \hat{\rho}) \mid \mathbf{y} \in \mathbb{Y}_2)$ is so small that the true permutation p -value $p(\mathbf{y}_0, \hat{\rho})$ must be of the same order of magnitude as the estimate $\hat{p}_2 \equiv \mathbb{E}(p(\mathbf{y}, \hat{\rho}) \mid \mathbf{y} \in \mathbb{Y}_2)$ that we study at length.

We obtain \hat{p}_2 and the mean square discrepancy over its reference distribution by further extending Brauchart and Dick's generalization of Stolarsky's invariance. More generally, we can replace the constraint $\langle \mathbf{y}, \mathbf{x}_0 \rangle = \langle \mathbf{y}_0, \mathbf{x}_0 \rangle$ by $\langle \mathbf{y}, \mathbf{x}_c \rangle = \langle \mathbf{y}_0, \mathbf{x}_c \rangle$ for any individual $c \in \{0, 1, \dots, N-1\}$. Our estimate \hat{p}_3 takes \mathbf{x}_c to be whichever permuted point \mathbf{x}_k happens to be closest to \mathbf{y}_0 .

Smaller sets \mathbb{Y} could be even better than \mathbb{Y}_2 . In the extreme, if we could work with \mathbb{Y} that satisfies $\langle \mathbf{y}, \mathbf{x}_k \rangle = \langle \mathbf{y}_0, \mathbf{x}_k \rangle$, for all $0 \leq k < N$ then all $\mathbf{y} \in \mathbb{Y}$ would have $p(\mathbf{y}, \hat{\rho}) = p(\mathbf{y}_0, \hat{\rho}) = p$ and the mean over $\mathbf{y} \in \mathbb{Y}$ would have no error. Any smaller set is only useful if we can efficiently compute with it.

Although we found these results via invariance, we can also obtain them via probabilistic arguments. As a consequence we have a probabilistic derivation of Stolarsky's formula. Bilyk et al. (2016) have independently found this connection. Some of our results are for arbitrary \mathbf{x} , but our best computational formulas are for the case where the variable \mathbf{x} is binary, as it is for the Parkinson's disease data sets.

Outline

The rest of the paper is organized as follows. Section 2 presents some context on permutation tests and gives some results from spherical geometry. In Section 3 we use Stolarsky's invariance principle as generalized by Brauchart and

Dick (2013) to obtain the mean squared error between the true p -value and its continuous approximation \hat{p}_1 , averaging over all spherical caps of volume \hat{p}_1 . This section also has a probabilistic derivation of that mean squared error. In Section 4 we describe some finer approximations \tilde{p} for the p -value. These use the set \mathbb{Y}_2 to condition on not just the volume of the spherical cap but also on its distance from the original data point \mathbf{x}_0 , or from some other point, such as the closest permutation of \mathbf{x}_0 to \mathbf{y}_0 . By always including the original point we ensure that $\tilde{p} \geq 1/N$. That is a desirable property because the true permutation p -value cannot be smaller than $1/N$. In Section 5 we modify the proof in Brauchart and Dick (2013), to further generalize their invariance results to include the mean squared error of the finer approximations. Section 6 extends our estimates to two-sided testing. Section 7 illustrates our p -value approximations numerically. We see that an RMS error in the estimate \hat{p}_2 is of the same order of magnitude as \hat{p}_2 itself. That is, \hat{p}_2 has a relative error property like saddlepoint estimates do. Section 8 makes a numerical comparison to saddlepoint methods in simulated data. The saddlepoint estimates come out more accurate than \hat{p}_2 but are biased low in the simulated examples. Section 9 compares the accuracy of our approximations to each other and to the saddlepoint approximation for 6180 gene sets and some Parkinson’s disease data sets. In the data examples, the new approximations come out closer to some gold standard estimates (based on large Monte Carlo samples) than the saddlepoint estimates do, which once again are biased low. From Table 6.3 of He (2016), the saddlepoint computations take roughly 30 times longer than \hat{p}_2 does. Section 10 draws some conclusions and discusses the challenges in getting a computationally feasible p -value that accounts for both sampling uncertainty of (\mathbf{x}, \mathbf{y}) and the uncertainty in \hat{p} as an estimate of p . Most of the proofs are in the Appendix, Section 11.

Software

The proposed approximations are implemented in the R package pipeGS on CRAN. Given a binary input label and a gene expression measurement matrix, it computes our three p value approximations for the linear gene set statistics. Those statistics, \hat{p}_1 , \hat{p}_2 , \hat{p}_3 , are mentioned above and then presented in more detail in Section 4. We provide an implementation of the saddlepoint approximation in the package as well.

2. Background and notation

The raw data contain points (X_i, Y_i) for $i = 1, \dots, n$, where Y_i may be a composite quantity derived from all Y_{gi} for g belonging to a gene set G , such as $Y_i = Y_{G_i}$ just before (1.2). We center and scale vectors (X_1, X_2, \dots, X_n) and (Y_1, Y_2, \dots, Y_n) yielding $\mathbf{x}_0, \mathbf{y}_0 \in \mathbb{S}^d$ for $d = n - 1$. Both points belong to $\{\mathbf{z} \in \mathbb{S}^{n-1} \mid \mathbf{z}^\top \mathbf{1}_n = 0\}$. We can use an orthogonal matrix to rotate the points of this set onto $\mathbb{S}^{n-2} \times \{0\}$. As a result, we may simply work with $\mathbf{x}_0, \mathbf{y}_0 \in \mathbb{S}^d$ where $d = n - 2$.

The sample correlation of these variables is $\hat{\rho} = \mathbf{x}_0^\top \mathbf{y}_0 = \langle \mathbf{x}_0, \mathbf{y}_0 \rangle$. We use $\langle \mathbf{x}_0, \mathbf{y}_0 \rangle$ when we find that geometrical thinking is appropriate and to conform with [Brauchart and Dick \(2013\)](#). We use $\mathbf{x}_0^\top \mathbf{y}_0$ to emphasize computational or algebraic connotations.

Here we develop approximations to the one-sided p -value as that simplifies notation. Section 6 shows how to obtain the corresponding two-sided p -values. We assume that $\hat{\rho} > 0$ for otherwise \hat{p}_1 is going to be too large to be interesting. For instance with $m_0 = m_1$, $\hat{\rho} \leq 0$ implies that $\hat{p}_1 \geq 1/2$.

Our proposals are computationally most attractive in the case where X_i takes on just two values, such as 0 and 1. Then $\hat{\rho}$ is a two-sample test statistic for a difference in means. When there are m_0 observations with $X_i = 0$ and m_1 with $X_i = 1$ then \mathbf{x}_0 contains m_0 components equal to $-\sqrt{m_1/(nm_0)}$ and m_1 components equal to $+\sqrt{m_0/(nm_1)}$. Computational costs are often sensitive to the smaller sample size, $\underline{m} \equiv \min(m_0, m_1)$.

For this two-sample case there are only $N = \binom{m_0+m_1}{m_0}$ distinct permutations of \mathbf{x}_0 . We have called these $\mathbf{x}_0, \mathbf{x}_1, \dots, \mathbf{x}_{N-1}$ and the true p value is $p = (1/N) \sum_{k=0}^{N-1} \mathbf{1}(\mathbf{x}_k^\top \mathbf{y}_0 \geq \hat{\rho}) = (1/N) \sum_{k=0}^{N-1} \mathbf{1}(\mathbf{x}_k \in C(\mathbf{y}_0; \hat{\rho}))$.

Now suppose that there are exactly r indices for which \mathbf{x}_k is positive and \mathbf{x}_ℓ is negative. There are then r indices with the reverse pattern too. We say that \mathbf{x}_k and \mathbf{x}_ℓ are at ‘swap distance r ’ because r zeros from \mathbf{x}_k swapped positions with ones to yield \mathbf{x}_ℓ . In that case we easily find that

$$u(r) \equiv \langle \mathbf{x}_k, \mathbf{x}_\ell \rangle = 1 - r \left(\frac{1}{m_0} + \frac{1}{m_1} \right). \quad (2.1)$$

We need some geometric properties of the unit sphere and spherical caps. The surface volume of \mathbb{S}^d is $\omega_d = 2\pi^{(d+1)/2}/\Gamma((d+1)/2)$. We use σ_d for the volume element in \mathbb{S}^d normalized so that $\sigma_d(\mathbb{S}^d) = 1$. The spherical cap $C(\mathbf{y}; t) = \{\mathbf{z} \in \mathbb{S}^d \mid \mathbf{z}^\top \mathbf{y} \geq t\}$ has volume

$$\sigma_d(C(\mathbf{y}; t)) = \begin{cases} \frac{1}{2} I_{1-t^2} \left(\frac{d}{2}, \frac{1}{2} \right), & 0 \leq t \leq 1 \\ 1 - \frac{1}{2} I_{1-t^2} \left(\frac{d}{2}, \frac{1}{2} \right), & -1 \leq t < 0 \end{cases}$$

where $I_t(a, b)$ is the incomplete beta function

$$I_t(a, b) = \frac{1}{B(a, b)} \int_0^t x^{a-1} (1-x)^{b-1} dx$$

with $B(a, b) = \int_0^1 x^{a-1} (1-x)^{b-1} dx$. Obviously, this volume is 0 if $t < -1$ and it is 1 if $t > 1$. This volume is independent of \mathbf{y} so we may write $\sigma_d(C(\cdot, t))$ for the volume.

Our first approximation of the p -value is $\hat{p}_1(\hat{\rho}) = \sigma_d(C(\mathbf{y}; \hat{\rho}))$. We remarked earlier that this approximation equates a discrete fraction to a volume ratio. We show in Proposition 2 that $\hat{p}_1 = \mathbb{E}(p \mid \langle \mathbf{x}_0, \mathbf{y} \rangle = \hat{\rho})$ for $\mathbf{y} \sim \mathbf{U}(\mathbb{S}^d)$ as \mathbf{y}_0 would if the original Y_i were IID Gaussian. In Theorem 4, we find $\text{Var}(\hat{p}_1)$ under this assumption.

We frequently need to project $\mathbf{y} \in \mathbb{S}^d$ onto a point $\mathbf{x} \in \mathbb{S}^d$. In this representation $\mathbf{y} = t\mathbf{x} + \sqrt{1-t^2}\mathbf{y}^*$ where $t = \mathbf{y}^\top \mathbf{x} \in [-1, 1]$ and $\mathbf{y}^* \in \{\mathbf{z} \in \mathbb{S}^d \mid \mathbf{z}^\top \mathbf{x} = 0\}$ which is isomorphic to \mathbb{S}^{d-1} . The coordinates t and \mathbf{y}^* are unique. From equation (A.1) in Brauchart and Dick (2013) we get

$$d\sigma_d(\mathbf{y}) = \frac{\omega_{d-1}}{\omega_d} (1-t^2)^{d/2-1} dt d\sigma_{d-1}(\mathbf{y}^*). \quad (2.2)$$

In their case \mathbf{x} was $(0, 0, \dots, 1)$.

The intersection of two spherical caps of common height t is

$$C_2(\mathbf{x}, \mathbf{y}; t) \equiv C(\mathbf{x}; t) \cap C(\mathbf{y}; t).$$

We will need the volume of this intersection. Lee and Kim (2014) give a general solution for spherical cap intersections without requiring equal heights. They enumerate 25 cases, but our case does not correspond to any single case of theirs and so we obtain the formula we need directly, below. We suspect it must be known already, but we were unable to find it in the literature.

Lemma 1. *Let $\mathbf{x}, \mathbf{y} \in \mathbb{S}^d$ and $-1 \leq t \leq 1$ and put $u = \mathbf{x}^\top \mathbf{y}$. Let $V_2(u; t, d) = \sigma_d(C_2(\mathbf{x}, \mathbf{y}; t))$. If $u = 1$, then $V_2(u; t, d) = \sigma_d(C(\mathbf{x}; t))$. If $-1 < u < 1$, then*

$$V_2(u; t, d) = \frac{\omega_{d-1}}{\omega_d} \int_t^1 (1-s^2)^{\frac{d}{2}-1} \sigma_{d-1}(C(\mathbf{y}^*; \rho(s))) ds, \quad (2.3)$$

where $\rho(s) = (t - su) / \sqrt{(1-s^2)(1-u^2)}$. Finally, for $u = -1$,

$$V_2(u; t, d) = \begin{cases} 0, & t \geq 0 \\ \frac{\omega_{d-1}}{\omega_d} \int_{-|t|}^{|t|} (1-s^2)^{\frac{d}{2}-1} ds, & \text{else.} \end{cases} \quad (2.4)$$

Proof. Let $\mathbf{z} \sim \mathbf{U}(\mathbb{S}^d)$. Then $V_2(u; t, d) = \sigma_d(C_2(\mathbf{x}, \mathbf{y}; t)) = \Pr(\mathbf{z} \in C_2(\mathbf{x}, \mathbf{y}; t))$. If $u = 1$ then $\mathbf{x} = \mathbf{y}$ and so $C_2(\mathbf{x}, \mathbf{y}; t) = C(\mathbf{x}; t)$. For $u < 1$, we project \mathbf{y} and \mathbf{z} onto \mathbf{x} , via $\mathbf{z} = s\mathbf{x} + \sqrt{1-s^2}\mathbf{z}^*$ and $\mathbf{y} = u\mathbf{x} + \sqrt{1-u^2}\mathbf{y}^*$. Now

$$\begin{aligned} V_2(u; t, d) &= \int_{\mathbb{S}^d} \mathbf{1}(\langle \mathbf{x}, \mathbf{z} \rangle \geq t) \mathbf{1}(\langle \mathbf{y}, \mathbf{z} \rangle \geq t) d\sigma(\mathbf{z}) \\ &= \int_{-1}^1 \mathbf{1}(s \geq t) \frac{\omega_{d-1}}{\omega_d} (1-s^2)^{\frac{d}{2}-1} \\ &\quad \times \int_{\mathbb{S}^{d-1}} \mathbf{1}(su + \sqrt{1-s^2}\sqrt{1-u^2} \langle \mathbf{y}^*, \mathbf{z}^* \rangle \geq t) d\sigma_{d-1}(\mathbf{z}^*) ds. \end{aligned}$$

If $u > -1$ then this reduces to (2.3). For $u = -1$ we get

$$V_2(u; t, d) = \frac{\omega_{d-1}}{\omega_d} \int_{-1}^1 \mathbf{1}(s \geq t) \mathbf{1}(-s \geq t) (1-s^2)^{\frac{d}{2}-1} ds.$$

which reduces to (2.4). \square

When we give probabilistic arguments and interpretations we do so for a random center \mathbf{y} of a spherical cap. That random center is taken from two reference distributions. Those are distributions 1 and 2 below. Reference distribution 1 is illustrated in Figure 1. Distribution 2 is illustrated in Figure 2 of Section 4 where we first use it.

Reference distribution 1. *The vector $\mathbf{y} \sim \mathbf{U}(\mathbb{Y}_1)$ where $\mathbb{Y}_1 = \mathbb{S}^d$. Expectation under this distribution is denoted $\mathbb{E}_1(\cdot)$.*

Reference distribution 2. *The vector $\mathbf{y} \sim \mathbf{U}(\mathbb{Y}_2)$ where*

$$\mathbb{Y}_2 = \{\mathbf{z} \in \mathbb{S}^d \mid \mathbf{z}^\top \mathbf{x}_c = \tilde{\rho}\},$$

for some $-1 \leq \tilde{\rho} \leq 1$, and $c \in \{0, 1, \dots, N-1\}$. Then $\mathbf{y} = \tilde{\rho} \mathbf{x}_c + \sqrt{1 - \tilde{\rho}^2} \mathbf{y}^*$ for \mathbf{y}^* uniformly distributed on a subset of \mathbb{S}^d isomorphic to \mathbb{S}^{d-1} . Expectation under this distribution is denoted $\mathbb{E}_2(\cdot)$.

Reference distribution 1 holds true if the Y_i are IID Gaussian random variables (with positive variance). In that case, the estimate $\hat{\rho}_1$ is the same as we would get under a t -test. Reference distribution 2 is a significant narrowing of reference distribution 1 in the direction of the ultimate reference distribution: a point mass on $\mathbf{y} = \mathbf{y}_0$.

3. Approximation via spherical cap volume

Here we study the approximate p -value $\hat{\rho}_1(\hat{\rho}) = \sigma_d(C(\mathbf{y}; \hat{\rho}))$. First we find the mean squared error of this approximation over all spherical caps of the given volume via invariance. Next we give a probabilistic interpretation which includes the conditional unbiasedness result in Proposition 2 below. Then we give two computational simplifications, first taking advantage of the permutation structure of our points, and then second for permutations of a binary vector. We begin by restating the invariance principle.

Theorem 1. *Let $\mathbf{x}_0, \dots, \mathbf{x}_{N-1}$ be any points in \mathbb{S}^d . Then*

$$\begin{aligned} \frac{1}{N^2} \sum_{k, \ell=0}^{N-1} \|\mathbf{x}_k - \mathbf{x}_\ell\| + \frac{1}{C_d} \int_{-1}^1 \int_{S_d} \left| \sigma_d(C(\mathbf{z}; t)) - \frac{1}{N} \sum_{k=0}^{N-1} \mathbf{1}_{C(\mathbf{z}; t)}(\mathbf{x}_k) \right|^2 d\sigma_d(\mathbf{z}) dt \\ = \int_{\mathbb{S}^d} \int_{\mathbb{S}^d} \|\mathbf{x} - \mathbf{y}\| d\sigma_d(\mathbf{x}) d\sigma_d(\mathbf{y}) \end{aligned}$$

where $C_d = \omega_{d-1}/(d\omega_d)$.

Proof. [Stolarsky \(1973\)](#). □

[Brauchart and Dick \(2013\)](#) gave a simple proof of Theorem 1 using reproducing kernel Hilbert spaces. They also generalized Theorem 1 as follows.

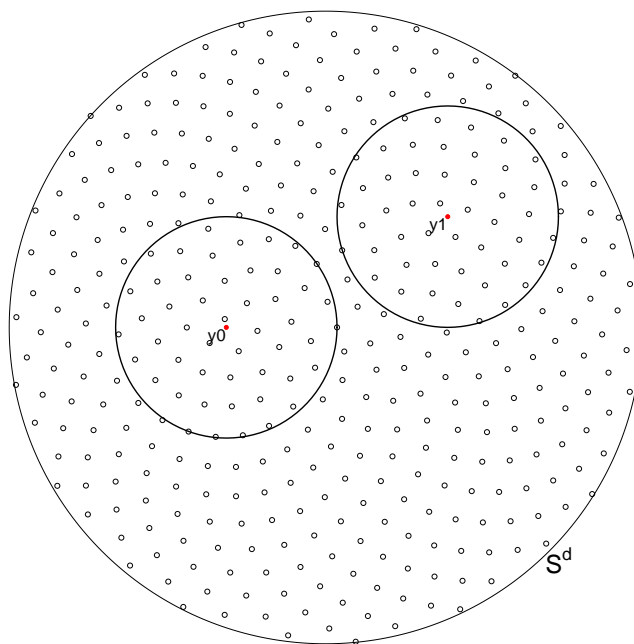


Fig 1: Illustration for reference distribution 1. The point \mathbf{y} is uniformly distributed over \mathbb{S}^d . The small open circles represent permuted vectors \mathbf{x}_k . The point \mathbf{y}_0 is the observed value of \mathbf{y} . The circle around it goes through \mathbf{x}_0 and represents a spherical cap of height $\mathbf{y}_0^\top \mathbf{x}_0$. A second spherical cap of equal volume is centered at $\mathbf{y} = \mathbf{y}_1$. We study moments of $p(\mathbf{y}, \hat{\rho})$, the fraction of \mathbf{x}_k in the cap centered at random \mathbf{y} .

Theorem 2. Let $\mathbf{x}_0, \dots, \mathbf{x}_{N-1}$ be any points in \mathbb{S}^d . Let $v : [-1, 1] \rightarrow (0, \infty)$ be any function with an antiderivative. Then

$$\begin{aligned} & \int_{-1}^1 v(t) \int_{\mathbb{S}^d} \left| \sigma_d(C(\mathbf{z}; t)) - \frac{1}{N} \sum_{k=0}^{N-1} \mathbf{1}_{C(\mathbf{z}; t)}(\mathbf{x}_k) \right|^2 d\sigma_d(\mathbf{z}) dt \\ &= \frac{1}{N^2} \sum_{k, l=0}^{N-1} K_v(\mathbf{x}_k, \mathbf{x}_l) - \int_{\mathbb{S}^d} \int_{\mathbb{S}^d} K_v(\mathbf{x}, \mathbf{y}) d\sigma_d(\mathbf{x}) d\sigma_d(\mathbf{y}) \end{aligned} \quad (3.1)$$

where $K_v(\mathbf{x}, \mathbf{y})$ is a reproducing kernel function defined by

$$K_v(\mathbf{x}, \mathbf{y}) = \int_{-1}^1 v(t) \int_{\mathbb{S}^d} \mathbf{1}_{C(\mathbf{z}; t)}(\mathbf{x}) \mathbf{1}_{C(\mathbf{z}; t)}(\mathbf{y}) d\sigma_d(\mathbf{z}) dt. \quad (3.2)$$

Proof. See Theorem 5.1 in Brauchart and Dick (2013) □

If we set $v(t) = 1$ and $K(\mathbf{x}, \mathbf{y}) = 1 - C_d \|\mathbf{x} - \mathbf{y}\|$, then we recover the original Stolarsky formula. Note that the statement of Theorem 5.1 in Brauchart and

Dick (2013) has a sign error in their counterpart to (3.1). The corrected statement (3.1) can be verified by comparing equations (5.3) and (5.4) of Brauchart and Dick (2013).

We would like a version of (3.1) just for one value of t such as $t = \hat{\rho} = \mathbf{x}_0^\top \mathbf{y}_0$. For $\hat{\rho} \in [-1, 1]$ and $\boldsymbol{\epsilon} = (\epsilon_1, \epsilon_2) \in (0, 1)^2$, let

$$v_{\boldsymbol{\epsilon}}(t) = \epsilon_2 + \frac{1}{\epsilon_1} \mathbf{1}(\hat{\rho} \leq t \leq \hat{\rho} + \epsilon_1). \quad (3.3)$$

Each $v_{\boldsymbol{\epsilon}}$ satisfies the conditions of Theorem 2 making (3.1) an identity in $\boldsymbol{\epsilon}$. We let $\epsilon_2 \rightarrow 0$ and then $\epsilon_1 \rightarrow 0$ on both sides of (3.1) for $v = v_{\boldsymbol{\epsilon}}$ yielding Theorem 3.

Theorem 3. *Let $\mathbf{x}_0, \mathbf{x}_1, \dots, \mathbf{x}_{N-1} \in \mathbb{S}^d$ and $t \in [-1, 1]$. Then*

$$\int_{\mathbb{S}^d} |p(\mathbf{y}, t) - \hat{p}_1(t)|^2 d\sigma_d(\mathbf{y}) = \frac{1}{N^2} \sum_{k=0}^{N-1} \sum_{\ell=0}^{N-1} \sigma_d(C_2(\mathbf{x}_k, \mathbf{x}_\ell; t)) - \hat{p}_1(t)^2. \quad (3.4)$$

Proof. See Section 11.1 of the Appendix which uses the limit argument described above. \square

We now give a proposition that holds for all distributions of $\mathbf{y} \in \mathbb{S}^d$ including our reference distributions 1 and 2.

Proposition 1. *For a random point $\mathbf{y} \in \mathbb{S}^d$,*

$$\mathbb{E}(p(\mathbf{y}, t)) = \frac{1}{N} \sum_{k=0}^{N-1} \Pr(\mathbf{y} \in C(\mathbf{x}_k; t)), \quad \text{and} \quad (3.5)$$

$$\mathbb{E}(p(\mathbf{y}, t)^2) = \frac{1}{N^2} \sum_{k, \ell=0}^{N-1} \Pr(\mathbf{y} \in C_2(\mathbf{x}_k, \mathbf{x}_\ell; t)). \quad (3.6)$$

Proposition 2. *For any $\mathbf{x}_0, \dots, \mathbf{x}_{N-1} \in \mathbb{S}^d$ and $t \in [-1, 1]$, $\hat{p}_1(t) = \mathbb{E}_1(p(\mathbf{y}, t))$.*

Proof. $\mathbb{E}_1(p(\mathbf{y}, t)) = \mathbb{E}_1\left[\frac{1}{N} \sum_{k=0}^{N-1} \mathbf{1}_{C(\mathbf{y}; t)}(\mathbf{x}_k)\right] = \sigma_d(C_d(\mathbf{y}; t)) = \hat{p}_1(t)$. \square

Combining Propositions 1 and 2 with Theorem 3 we find that if $\mathbf{y} \sim \mathbf{U}(\mathbb{S}^d)$, as it would for IID Gaussian Y_i , then $p(\mathbf{y}, \hat{\rho})$ is a random variable with mean $\hat{p}_1(\hat{\rho})$ and variance given by (3.4) with $t = \hat{\rho}$. Here $\hat{\rho} = \mathbf{x}_0^\top \mathbf{y}_0$ is fixed while \mathbf{y} is random.

The right hand side of (3.4) sums $O(N^2)$ terms. In a permutation analysis we might have $N = n!$ or $N = \binom{m_0+m_1}{m_0}$ for binary X_i , and so the computational cost could be high. The symmetry in a permutation set allows us to use

$$\int_{\mathbb{S}^d} |p(\mathbf{y}, t) - \hat{p}_1(t)|^2 d\sigma_d(\mathbf{y}) = \frac{1}{N} \sum_{k=0}^{N-1} \sigma_d(C_2(\mathbf{x}_0, \mathbf{x}_k; t)) - \hat{p}_1(t)^2$$

instead. This expression costs $O(N)$, the same as the full permutation analysis. The cost can be reduced for binary X_i .

When the X_i are binary, then for fixed t , $\sigma_d(C_2(\mathbf{x}_k, \mathbf{x}_\ell; t))$ just depends on the swap distance r between \mathbf{x}_k and \mathbf{x}_ℓ . Then

$$\int_{\mathbb{S}^d} |p(\mathbf{y}, t) - \hat{p}_1(t)|^2 d\sigma_d(\mathbf{y}) = \frac{1}{N} \sum_{r=0}^{\underline{m}} N_r V_2(u(r); t, d) - \hat{p}_1(t)^2 \quad (3.7)$$

for $V_2(u(r); t, d)$ given in Lemma 1, where $N_r = \sum_{k=0}^{N-1} \sum_{\ell=0}^{N-1} \mathbf{1}(r_{k,\ell} = r)$ counts pairs $(\mathbf{x}_k, \mathbf{x}_\ell)$ at swap distance r .

Theorem 4. *Let $\mathbf{x}_0 \in \mathbb{S}^d$ be the centered and scaled vector from an experiment with binary X_i of which m_0 are negative and m_1 are positive. Let $\mathbf{x}_0, \mathbf{x}_1, \dots, \mathbf{x}_{N-1}$ be the $N = \binom{m_0+m_1}{m_0}$ distinct permutations of \mathbf{x}_0 . If $\mathbf{y} \sim \mathbf{U}(\mathbb{S}^d)$, then for $t \in [-1, 1]$, and with $u(r)$ defined in (2.1),*

$$\begin{aligned} \mathbb{E}(p(\mathbf{y}, t)) &= \sigma_d(C(\mathbf{y}_0; t)), \quad \text{and} \\ \text{Var}(p(\mathbf{y}, t)) &= \frac{1}{N} \sum_{r=0}^{\underline{m}} \binom{m_0}{r} \binom{m_1}{r} V_2(u(r); t, d) - \hat{p}_1(t)^2. \end{aligned}$$

Proof. There are $\binom{m_0}{r} \binom{m_1}{r}$ permuted points \mathbf{x}_i at swap distance r from \mathbf{x}_0 . \square

4. A finer approximation to the p -value

In the previous section, we studied the distribution of permutation p -values $p(\mathbf{y}, t)$ with spherical cap centers $\mathbf{y} \sim \mathbf{U}(\mathbb{S}^d)$ and heights $t = \hat{\rho}$. In this section, we use reference distribution 2 to obtain a finer approximation to $p(\mathbf{y}_0, \hat{\rho})$ by studying the distribution of the p -values with centers \mathbf{y} satisfying the constraint $\langle \mathbf{y}, \mathbf{x}_0 \rangle = \langle \mathbf{y}_0, \mathbf{x}_0 \rangle = \hat{\rho}$. That is \mathbf{y} has reference distribution 2, which is $\mathbf{U}(\mathbb{Y}_2)$.

Our methods also let us impose the constraint $\langle \mathbf{y}, \mathbf{x}_c \rangle = \langle \mathbf{y}_0, \mathbf{x}_c \rangle \equiv \tilde{\rho}$ for any $c = 0, 1, 2, \dots, N-1$ that we like. Conditioning on $\langle \mathbf{y}, \mathbf{x}_c \rangle = \tilde{\rho}$ eliminates many irrelevant \mathbf{y} from consideration. In addition to our estimate \hat{p}_2 obtained by $\mathbf{x}_c = \mathbf{x}_0$, we consider a second choice. It is to choose \mathbf{x}_c to be the closest permutation of \mathbf{x}_0 to \mathbf{y}_0 . That is $c = \arg \max_k \langle \mathbf{y}_0, \mathbf{x}_k \rangle$.

For an index $c \in \{0, 1, \dots, N-1\}$ conditioning as above leads to

$$\tilde{p}_c = \mathbb{E}_2(p(\mathbf{y}, \hat{\rho})) = \mathbb{E}_1(p(\mathbf{y}, \hat{\rho}) \mid \mathbf{y}^\top \mathbf{x}_c = \mathbf{y}_0^\top \mathbf{x}_c), \quad (4.1)$$

and our two special cases are

$$\hat{p}_2 \equiv \tilde{p}_0, \quad \text{and} \quad \hat{p}_3 \equiv \tilde{p}_c, \quad \text{where} \quad c = \arg \max_{0 \leq k < N} \langle \mathbf{y}_0, \mathbf{x}_k \rangle. \quad (4.2)$$

For an illustration of reference distribution 2 see Figure 2.

Notice that \hat{p}_2 cannot go below $1/N$ because all of the points \mathbf{y} that it includes have $\mathbf{x}_0 \in C(\mathbf{y}; \hat{\rho})$. In fact \mathbf{x}_0 is on the boundary of this spherical cap. Since the true value satisfies $p \geq 1/N$, having $\hat{p}_2 \geq 1/N$ is a desirable property. Similarly, $\hat{p}_3 \geq 1/N$ because then \mathbf{x}_c is in general an interior point of $C(\mathbf{y}, \hat{\rho})$. We expect

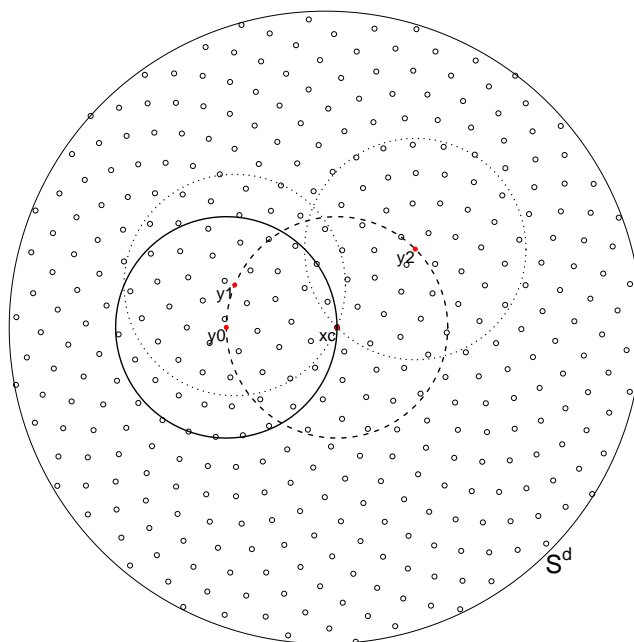


Fig 2: Illustration for reference distribution 2. The original response vector is \mathbf{y}_0 with $\mathbf{y}_0^\top \mathbf{x}_0 = \hat{\rho}$ and \mathbf{x}_0 marked \mathbf{x}_c . We consider alternative \mathbf{y} uniformly distributed on the surface of $C(\mathbf{x}_0; \hat{\rho})$ (dashed circle) with examples \mathbf{y}_1 and \mathbf{y}_2 . Around each such \mathbf{y}_j there is a spherical cap of height $\hat{\rho}$ that just barely includes $\mathbf{x}_c = \mathbf{x}_0$. The small open circles are permuted points \mathbf{x}_k . The fraction of those open circles that belong to the spherical cap $C(\mathbf{y}, \hat{\rho})$ is $p(\mathbf{y}, \hat{\rho})$. We use $\hat{\rho}_2 = \mathbb{E}_2(p(\mathbf{y}, \hat{\rho}))$ and find an expression for $\mathbb{E}_2((\hat{\rho}_2 - p(\mathbf{y}, \hat{\rho}))^2)$.

that $\hat{\rho}_3$ should be more conservative than $\hat{\rho}_2$ and we see this numerically in Section 7.

From Proposition 1, we can get our estimate \tilde{p}_c and its mean squared error by finding single and double inclusion probabilities for \mathbf{y} .

To compute \tilde{p}_c we need to sum N values $\Pr(\mathbf{y} \in C(\mathbf{x}_k; t) \mid \mathbf{y}^\top \mathbf{x}_c = \hat{\rho})$ and for \tilde{p}_c to be useful we must compute it in $o(N)$ time. The computations are feasible in the binary case (X_i at two levels), which we now focus on.

Let $u_j = \mathbf{x}_j^\top \mathbf{x}_0$ for $j = 1, 2$, and let $u_3 = \mathbf{x}_1^\top \mathbf{x}_2$. Let the projection of \mathbf{y} on \mathbf{x}_c be $\mathbf{y} = \tilde{\rho} \mathbf{x}_c + \sqrt{1 - \tilde{\rho}^2} \mathbf{y}^*$. Then the single and double point inclusion probabilities under reference distribution 2 are

$$P_1(u_1, \tilde{\rho}, \hat{\rho}) = \int_{\mathbb{S}^{d-1}} \mathbf{1}(\langle \mathbf{y}, \mathbf{x}_1 \rangle \geq \hat{\rho}) d\sigma_{d-1}(\mathbf{y}^*), \quad \text{and} \quad (4.3)$$

$$P_2(u_1, u_2, u_3, \tilde{\rho}, \hat{\rho}) = \int_{\mathbb{S}^{d-1}} \mathbf{1}(\langle \mathbf{y}, \mathbf{x}_1 \rangle \geq \hat{\rho}) \mathbf{1}(\langle \mathbf{y}, \mathbf{x}_2 \rangle \geq \hat{\rho}) d\sigma_{d-1}(\mathbf{y}^*) \quad (4.4)$$

where $\hat{\rho} = \langle \mathbf{x}_0, \mathbf{y}_0 \rangle$. If two permutations of \mathbf{x}_0 are at swap distance r , then their inner product is $u(r) = 1 - r(m_0^{-1} + m_1^{-1})$ from equation (2.1).

Lemma 2. *Let the projection of \mathbf{x}_1 onto \mathbf{x}_c be $\mathbf{x}_1 = u_1 \mathbf{x}_c + \sqrt{1 - u_1^2} \mathbf{x}_1^*$. Then the single point inclusion probability from (4.3) is*

$$P_1(u_1, \tilde{\rho}, \hat{\rho}) = \begin{cases} \mathbf{1}(\tilde{\rho} u_1 \geq \hat{\rho}), & u_1 = \pm 1 \text{ or } \tilde{\rho} = \pm 1 \\ \sigma_{d-1}(C(\mathbf{x}_1^*, \rho^*)), & u_1 \in (-1, 1), \tilde{\rho} \in (-1, 1) \end{cases} \quad (4.5)$$

where $\rho^* = (\hat{\rho} - \tilde{\rho} u_1) / \sqrt{(1 - \tilde{\rho}^2)(1 - u_1^2)}$.

Proof. The projection of \mathbf{y} onto \mathbf{x}_c is $\mathbf{y} = \tilde{\rho} \mathbf{x}_c + \sqrt{1 - \tilde{\rho}^2} \mathbf{y}^*$. Now

$$\langle \mathbf{y}, \mathbf{x}_1 \rangle = \begin{cases} \tilde{\rho} u_1, & u_1 = \pm 1 \text{ or } \tilde{\rho} = \pm 1 \\ \tilde{\rho} u_1 + \sqrt{1 - \tilde{\rho}^2} \sqrt{1 - u_1^2} \langle \mathbf{y}^*, \mathbf{x}_1^* \rangle, & u_1 \in (-1, 1), \tilde{\rho} \in (-1, 1) \end{cases}$$

and the result easily follows. \square

We can now give a computable expression for \tilde{p}_c and hence for \hat{p}_2 and \hat{p}_3 .

Theorem 5. *For $-1 \leq \hat{\rho} \leq 1$ and $-1 \leq \tilde{\rho} \leq 1$,*

$$\tilde{p}_c = \mathbb{E}_2(p(\mathbf{y}, \hat{\rho})) = \frac{1}{N} \sum_{r=0}^m \binom{m_0}{r} \binom{m_1}{r} P_1(u(r), \tilde{\rho}, \hat{\rho}) \quad (4.6)$$

where $u(r)$ is given in equation (2.1), $P_1(u(r), \tilde{\rho}, \hat{\rho})$ is given in equation (4.5) and $\tilde{\rho} = \mathbf{x}_c^\top \mathbf{y}_0$.

Proof. There are $\binom{m_0}{r} \binom{m_1}{r}$ permutations of \mathbf{x}_0 at swap distance r from \mathbf{x}_c . \square

From (4.6) we see that \tilde{p}_c can be computed in $O(\underline{m})$ work. The mean squared error for \tilde{p}_c is more complicated and will be more expensive. We need the double point inclusion probabilities and then we need to count the number of pairs $\mathbf{x}_k, \mathbf{x}_\ell$ forming a given set of swap distances among $\mathbf{x}_k, \mathbf{x}_\ell, \mathbf{x}_c$.

Lemma 3. *For $j = 1, 2$, let r_j be the swap distance of \mathbf{x}_j from \mathbf{x}_c and let r_3 be the swap distance between \mathbf{x}_1 and \mathbf{x}_2 . Let u_1, u_2, u_3 be the corresponding inner products given by (2.1). If there are equalities among $\mathbf{x}_1, \mathbf{x}_2$ and \mathbf{x}_c , then the double point inclusion probability from (4.4) is*

$$P_2(u_1, u_2, u_3, \tilde{\rho}, \hat{\rho}) = \begin{cases} \mathbf{1}(\tilde{\rho} \geq \hat{\rho}), & \mathbf{x}_1 = \mathbf{x}_2 = \mathbf{x}_c \\ \mathbf{1}(\tilde{\rho} \geq \hat{\rho}) P_1(u_2, \tilde{\rho}, \hat{\rho}), & \mathbf{x}_1 = \mathbf{x}_c \neq \mathbf{x}_2 \\ \mathbf{1}(\tilde{\rho} \geq \hat{\rho}) P_1(u_1, \tilde{\rho}, \hat{\rho}), & \mathbf{x}_2 = \mathbf{x}_c \neq \mathbf{x}_1 \\ P_1(u_2, \tilde{\rho}, \hat{\rho}), & \mathbf{x}_1 = \mathbf{x}_2 \neq \mathbf{x}_c. \end{cases}$$

If $\mathbf{x}_1, \mathbf{x}_2$ and \mathbf{x}_c are three distinct points with $\min(u_1, u_2) = -1$, then

$$P_2(u_1, u_2, u_3, \tilde{\rho}, \hat{\rho}) = \begin{cases} \mathbf{1}(-\tilde{\rho} \geq \hat{\rho}) P_1(u_2, \tilde{\rho}, \hat{\rho}), & u_1 = -1 \\ \mathbf{1}(-\tilde{\rho} \geq \hat{\rho}) P_1(u_1, \tilde{\rho}, \hat{\rho}), & u_2 = -1. \end{cases}$$

$$\begin{aligned}
 \mathbf{x}_c &= (\overbrace{+, +, +, +, +, \dots, +, +, +, +}^{m_1}, \overbrace{-, -, -, -, -, \dots, -, -, -, -}^{m_0}) \\
 \mathbf{x}_1 &= (\overbrace{+, +, +, \dots, +, -, -, -, \dots, -}^{m_1}, \overbrace{+, +, +, \dots, +, +, +, -, \dots, -}^{m_0}) \\
 &\quad \underbrace{\hspace{15em}}_{r_1} \\
 \mathbf{x}_2 &= (\overbrace{+, \dots, +, -, -, \dots, -, +, \dots, +}^{m_1}, \overbrace{-, \dots, -, +, +, \dots, +, -, \dots, -}^{m_0}) \\
 &\quad \underbrace{\hspace{15em}}_{r_2} \\
 &\quad \underbrace{\hspace{10em}}_{\delta_1} \qquad \underbrace{\hspace{10em}}_{\delta_2}
 \end{aligned}$$

Fig 3: Illustration of r_1 , r_2 , δ_1 and δ_2 . The points \mathbf{x}_c , \mathbf{x}_1 and \mathbf{x}_2 each have m_0 negative and m_1 positive components. For $j = 1, 2$ the swap distance between \mathbf{x}_j and \mathbf{x}_c is r_j . There are δ_1 positive components of \mathbf{x}_c where both \mathbf{x}_1 and \mathbf{x}_2 are negative, and δ_2 negative components of \mathbf{x}_c where both \mathbf{x}_j are positive.

Otherwise $-1 < u_1, u_2 < 1$, and then

$$\begin{aligned}
 &P_2(u_1, u_2, u_3, \tilde{\rho}, \hat{\rho}) \\
 &= \begin{cases} \mathbf{1}(\tilde{\rho}u_1 \geq \hat{\rho})\mathbf{1}(\tilde{\rho}u_2 \geq \hat{\rho}), & \tilde{\rho} = \pm 1 \\ \int_{-1}^1 \frac{\omega_{d-2}}{\omega_{d-1}} (1-t^2)^{\frac{d-1}{2}-1} \mathbf{1}(t \geq \rho_1) \mathbf{1}(tu_3^* \geq \rho_2) dt, & \tilde{\rho} \neq \pm 1, u_3^* = \pm 1 \\ \int_{-1}^1 \frac{\omega_{d-2}}{\omega_{d-1}} (1-t^2)^{\frac{d-1}{2}-1} \mathbf{1}(t \geq \rho_1) \sigma_{d-2} \left(C(\mathbf{x}_2^{**}, \frac{\rho_2 - tu_3^*}{\sqrt{1-t^2}\sqrt{1-u_3^{*2}}}) \right) dt, & \tilde{\rho} \neq \pm 1, |u_3^*| < 1 \end{cases}
 \end{aligned}$$

where

$$u_3^* = \frac{u_3 - u_1 u_2}{\sqrt{1-u_1^2}\sqrt{1-u_2^2}} \quad \text{and} \quad \rho_j = \frac{\hat{\rho} - \tilde{\rho}u_j}{\sqrt{1-\tilde{\rho}^2}\sqrt{1-u_j^2}}, \quad j = 1, 2 \quad (4.7)$$

and \mathbf{x}_2^{**} is the residual from the projection of \mathbf{x}_2^* on \mathbf{x}_1^* .

Proof. See Section 11.2. □

Next we consider the swap configuration among \mathbf{x}_1 , \mathbf{x}_2 and \mathbf{x}_c . Let \mathbf{x}_j be at swap distance r_j from \mathbf{x}_c , for $j = 1, 2$. We let δ_1 be the number of positive components of \mathbf{x}_c that are negative in both \mathbf{x}_1 and \mathbf{x}_2 . Similarly, δ_2 is the number of negative components of \mathbf{x}_c that are positive in both \mathbf{x}_1 and \mathbf{x}_2 . See Figure 3. The swap distance between \mathbf{x}_1 and \mathbf{x}_2 is then $r_3 = r_1 + r_2 - \delta_1 - \delta_2$.

Let $\mathbf{r} = (r_1, r_2)$, $\boldsymbol{\delta} = (\delta_1, \delta_2)$ and $\underline{r} = \min(r_1, r_2)$. We will study values of $r_1, r_2, r_3, \delta_1, \delta_2$ ranging over the following sets:

$$\begin{aligned}
 r_1, r_2 &\in R = \{1, \dots, \underline{m}\} \\
 \delta_1 &\in D_1(\mathbf{r}) = \{\max(0, r_1 + r_2 - m_0), \dots, \underline{r}\} \\
 \delta_2 &\in D_2(\mathbf{r}) = \{\max(0, r_1 + r_2 - m_1), \dots, \underline{r}\}, \quad \text{and} \\
 r_3 &\in R_3(\mathbf{r}) = \{\max(1, r_1 + r_2 - 2\underline{r}), \dots, \min(r_1 + r_2, \underline{m}, m_0 + m_1 - r_1 - r_2)\}.
 \end{aligned}$$

Whenever the lower bound for one of these sets exceeds the upper bound, we take the set to be empty, and a sum over it to be zero. Note that while $r_1 = 0$ is possible, it corresponds to $\mathbf{x}_1 = \mathbf{x}_c$ and we will handle that case specially, excluding it from R .

The number of pairs $(\mathbf{x}_\ell, \mathbf{x}_k)$ with a fixed \mathbf{r} and $\boldsymbol{\delta}$ is

$$c(\mathbf{r}, \boldsymbol{\delta}) = \binom{m_0}{\delta_1} \binom{m_1}{\delta_2} \binom{m_0 - \delta_1}{r_1 - \delta_1} \binom{m_1 - \delta_2}{r_1 - \delta_2} \binom{m_0 - r_1}{r_2 - \delta_1} \binom{m_1 - r_1}{r_2 - \delta_2}. \quad (4.8)$$

Then the number of configurations given r_1, r_2 and r_3 is

$$c(r_1, r_2, r_3) = \sum_{\delta_1 \in D_1} \sum_{\delta_2 \in D_2} c(\mathbf{r}, \boldsymbol{\delta}) \mathbf{1}(r_3 = r_1 + r_2 - \delta_1 - \delta_2). \quad (4.9)$$

We can now get an expression for the expected mean squared error under reference distribution 2 which combined with Theorem 5 for the mean provides an expression for the mean squared error of \tilde{p}_c .

Theorem 6. For $-1 \leq \hat{\rho} \leq 1$ and $-1 \leq \tilde{\rho} \leq 1$,

$$\begin{aligned} \mathbb{E}_2(p(\mathbf{y}, \hat{\rho})^2) &= \frac{1}{N^2} \left[\mathbf{1}(\tilde{\rho} \geq \hat{\rho}) + 2 \sum_{r=1}^{\underline{m}} \binom{m_0}{r} \binom{m_1}{r} P_2(1, u(r), u(r), \tilde{\rho}, \hat{\rho}) \right. \\ &\quad + \sum_{r=1}^{\underline{m}} \binom{m_0}{r} \binom{m_1}{r} P_1(u(r), \tilde{\rho}, \hat{\rho}) \\ &\quad \left. + \sum_{r_1 \in R} \sum_{r_2 \in R} \sum_{r_3 \in R_3(\mathbf{r})} c(r_1, r_2, r_3) P_2(u_1, u_2, u_3, \tilde{\rho}, \hat{\rho}) \right] \end{aligned} \quad (4.10)$$

where $P_2(\cdot)$ is the double inclusion probability in (4.4) and $c(r_1, r_2, r_3)$ is the configuration count in (4.9).

Proof. See Section 11.3 of the Appendix. \square

In our experience, the cost of computing $\mathbb{E}_2(p(\mathbf{y}, \hat{\rho})^2)$ under reference distribution 2 is dominated by the cost of the $O(\underline{m}^3)$ integrals required to get the $P_2(\cdot)$ values in (4.10). The cost also includes an $O(\underline{m}^4)$ component because $c(r_1, r_2, r_3)$ is also a sum of $O(\underline{m})$ terms, but it did not dominate the computation at the sample sizes we looked at (up to several hundred).

5. Generalized Stolarsky Invariance

Here we obtain the results for reference distribution 2 in a different way, by extending the work by Brauchart and Dick (2013). They introduced a weight on the height t of the spherical cap in the average. We now apply a weight function to the inner product $\langle \mathbf{z}, \mathbf{x}_c \rangle$ between the center \mathbf{z} of the spherical cap and a special point \mathbf{x}_c .

Theorem 7. Let $\mathbf{x}_0, \dots, \mathbf{x}_{N-1}$ be arbitrary points in \mathbb{S}^d and $v(\cdot)$ and $h(\cdot)$ be positive functions in $L_2([-1, 1])$. Then for any $\mathbf{x}' \in \mathbb{S}^d$, the following equation holds,

$$\begin{aligned} & \int_{-1}^1 v(t) \int_{\mathbb{S}^d} h(\langle \mathbf{z}, \mathbf{x}' \rangle) \left| \sigma_d(C(\mathbf{z}; t)) - \frac{1}{N} \sum_{k=0}^{N-1} \mathbf{1}_{C(\mathbf{z}; t)}(\mathbf{x}_k) \right|^2 d\sigma_d(\mathbf{z}) dt \\ &= \frac{1}{N^2} \sum_{k, \ell=0}^{N-1} K_{v, h, \mathbf{x}'}(\mathbf{x}_k, \mathbf{x}_\ell) + \int_{\mathbb{S}^d} \int_{\mathbb{S}^d} K_{v, h, \mathbf{x}'}(\mathbf{x}, \mathbf{y}) d\sigma_d(\mathbf{x}) d\sigma_d(\mathbf{y}) \\ & \quad - \frac{2}{N} \sum_{k=0}^{N-1} \int_{\mathbb{S}^d} K_{v, h, \mathbf{x}'}(\mathbf{x}, \mathbf{x}_k) d\sigma_d(\mathbf{x}) \end{aligned} \quad (5.1)$$

where $K_{v, h, \mathbf{x}'} : \mathbb{S}^d \times \mathbb{S}^d \rightarrow \mathbb{R}$ is a reproducing kernel defined by

$$K_{v, h, \mathbf{x}'}(\mathbf{x}, \mathbf{y}) = \int_{-1}^1 v(t) \int_{\mathbb{S}^d} h(\langle \mathbf{z}, \mathbf{x}' \rangle) \mathbf{1}_{C(\mathbf{z}; t)}(\mathbf{x}) \mathbf{1}_{C(\mathbf{z}; t)}(\mathbf{y}) d\sigma_d(\mathbf{z}) dt. \quad (5.2)$$

Proof. See Section 11.4 of the Appendix. \square

Remark. We will use this result for $\mathbf{x}' = \mathbf{x}_c$, where \mathbf{x}_c is one of the N given points. The theorem holds for general $\mathbf{x}' \in \mathbb{S}^d$, but the result is computationally and statistically more attractive when $\mathbf{x}' = \mathbf{x}_c$.

We now show that the second moment in Theorem 6 holds as a special limiting case of Theorem 7. In addition to v_ϵ from Section 3 we introduce $\boldsymbol{\eta} = (\eta_1, \eta_2) \in (0, 1)^2$ and

$$h_{\boldsymbol{\eta}}(s) = \eta_2 + \frac{1}{\eta_1 \binom{\omega_d - 1}{\omega_d} (1 - s^2)^{d/2 - 1}} \mathbf{1}(\tilde{\rho} \leq s \leq \tilde{\rho} + \eta_1) \quad (5.3)$$

Using these results we can now establish the following theorem, which provides the second moment of $p(\mathbf{y}, \hat{\rho})$ under reference distribution 2.

Theorem 8. Let $\mathbf{x}_0 \in \mathbb{S}^d$ be the centered and scaled vector from an experiment with binary X_i of which m_0 are negative and m_1 are positive. Let $\mathbf{x}_0, \mathbf{x}_1, \dots, \mathbf{x}_{N-1}$ be the $N = \binom{m_0 + m_1}{m_0}$ distinct permutations of \mathbf{x}_0 . Let \mathbf{x}_c be one of the \mathbf{x}_k and define $\tilde{\rho}_c$ by (4.1). Then

$$\mathbb{E}_2(\tilde{\rho}_c(\mathbf{y}, \hat{\rho})^2) = \frac{1}{N^2} \sum_{k, \ell=0}^{N-1} \int_{\mathbb{S}^{d-1}} \mathbf{1}(\langle \mathbf{y}, \mathbf{x}_k \rangle \geq \hat{\rho}) \mathbf{1}(\langle \mathbf{y}, \mathbf{x}_\ell \rangle \geq \hat{\rho}) d\sigma_{d-1}(\mathbf{y}^*)$$

where $\mathbf{y} = \tilde{\rho}_c \mathbf{x}_c + \sqrt{1 - \tilde{\rho}_c^2} \mathbf{y}^*$.

Proof. The proof uses Theorem 7 with a sequence of h defined in (5.3) and v defined in (3.3). See Section 11.5 of the appendix. \square

This result shows that we can use the invariance principle to derive the second moment of $p(\mathbf{y}, \hat{\rho})$ under reference distribution 2. The mean square in Theorem 8 is consistent with the second moment equation (3.6) in Proposition 1.

6. Two-sided p-values

In statistical applications it is more usual to report two-sided p -values. A conservative approach is to use $2 \min(p, 1 - p)$ where p is a one-sided p -value. A sharper choice is

$$p = \frac{1}{N} \sum_{k=0}^{N-1} \mathbf{1}(|\mathbf{x}_k^\top \mathbf{y}_0| \geq |\hat{\rho}|).$$

This choice changes our estimate under reference distribution 2. It also changes the second moment of our estimate \hat{p}_1 .

The two-sided version of the estimate $\hat{p}_1(\hat{\rho})$ is $2\sigma_d(C(\mathbf{y}; |\hat{\rho}|))$, the same as if we had doubled a one-sided estimate. Also $\mathbb{E}_1(p) = \hat{p}_1$ in the two-sided case. We now consider the mean square for the two-sided estimate under reference distribution 1. For $\mathbf{x}_1, \mathbf{x}_2 \in \mathbb{S}^d$ with $u = \mathbf{x}_1^\top \mathbf{x}_2$, the two-sided double inclusion probability under reference distribution 1 is

$$\tilde{V}_2(u; t, d) = \int_{\mathbb{S}^d} \mathbf{1}(|\mathbf{z}^\top \mathbf{x}_1| \geq |t|) \mathbf{1}(|\mathbf{z}^\top \mathbf{x}_2| \geq |t|) d\sigma_d(\mathbf{z}).$$

Writing $\mathbf{1}(|\mathbf{z}^\top \mathbf{x}_i| \geq |t|) = \mathbf{1}(\mathbf{z}^\top \mathbf{x}_k \geq |t|) + \mathbf{1}(\mathbf{z}^\top (-\mathbf{x}_k) \geq |t|)$ for $k = 1, 2$ and expanding the product, we get

$$\tilde{V}_2(u; t, d) = 2V_2(u; |t|, d) + 2V_2(-u; |t|, d).$$

By replacing $V_2(u, t, d)$ with $\tilde{V}_2(u, t, d)$ and $\hat{p}_1(t)$ with $2\sigma_d(C(\mathbf{y}; |t|))$ in Theorem 4, we get the variance of two-sided p -values under reference distribution 1.

To obtain corresponding formulas under reference distribution 2, we use the usual notation. Let $u_j = \mathbf{x}_j^\top \mathbf{x}_0$ for $j = 1, 2$, and let $u_3 = \mathbf{x}_1^\top \mathbf{x}_2$. Let the projection of \mathbf{y} on \mathbf{x}_c be $\mathbf{y} = \tilde{\rho} \mathbf{x}_c + \sqrt{1 - \tilde{\rho}^2} \mathbf{y}^*$. Now

$$\tilde{P}_1(u_1, \tilde{\rho}, \hat{\rho}) = \int_{\mathbb{S}^{d-1}} \mathbf{1}(|\langle \mathbf{y}, \mathbf{x}_1 \rangle| \geq |\hat{\rho}|) d\sigma_{d-1}(\mathbf{y}^*), \quad \text{and}, \quad (6.1)$$

$$\tilde{P}_2(u_1, u_2, u_3, \tilde{\rho}, \hat{\rho}) = \int_{\mathbb{S}^{d-1}} \mathbf{1}(|\langle \mathbf{y}, \mathbf{x}_1 \rangle| \geq |\hat{\rho}|) \mathbf{1}(|\langle \mathbf{y}, \mathbf{x}_2 \rangle| \geq |\hat{\rho}|) d\sigma_{d-1}(\mathbf{y}^*) \quad (6.2)$$

are the appropriate single and double inclusion probabilities.

After writing $\mathbf{1}(|\langle \mathbf{y}, \mathbf{x}_k \rangle| \geq |\hat{\rho}|) = \mathbf{1}(\langle \mathbf{y}, \mathbf{x}_k \rangle \geq |\hat{\rho}|) + \mathbf{1}(\langle \mathbf{y}, -\mathbf{x}_k \rangle \geq |\hat{\rho}|)$ for $k = 1, 2$ and expanding the product, we get

$$\begin{aligned} \tilde{P}_1(u_1, \tilde{\rho}, \hat{\rho}) &= P_1(u_1, \tilde{\rho}, |\hat{\rho}|) + P_1(-u_1, \tilde{\rho}, |\hat{\rho}|), \quad \text{and} \\ \tilde{P}_2(u_1, u_2, u_3, \tilde{\rho}, \hat{\rho}) &= P_2(u_1, u_2, u_3, \tilde{\rho}, |\hat{\rho}|) + P_2(-u_1, u_2, -u_3, \tilde{\rho}, |\hat{\rho}|) \\ &\quad + P_2(u_1, -u_2, -u_3, \tilde{\rho}, |\hat{\rho}|) + P_2(-u_1, -u_2, u_3, \tilde{\rho}, |\hat{\rho}|). \end{aligned}$$

Changing $P_1(u_1, \tilde{\rho}, \hat{\rho})$ and $P_2(u_1, u_2, u_3, \tilde{\rho}, \hat{\rho})$ to $\tilde{P}_1(u_1, \tilde{\rho}, \hat{\rho})$ and $\tilde{P}_2(u_1, u_2, u_3, \tilde{\rho}, \hat{\rho})$ respectively in Theorems 5 and 6, we get the first and second moments for two-sided p -values under reference distribution 2.

For a two-sided p -value, \hat{p}_3 is calculated with \mathbf{x}_c where $\tilde{c} = \arg \max_k |\langle \mathbf{y}_0, \mathbf{x}_k \rangle|$. For $m_0 = m_1$, $\tilde{c} = c = \arg \max_k \langle \mathbf{y}_0, \mathbf{x}_k \rangle$, but the result may differ significantly for unequal sample sizes.

7. Numerical Results

We consider two-sided p -values in this section. The main finding is that the root mean squared error (RMSE) of \hat{p}_2 under reference distribution 2 is usually just a small multiple of \hat{p}_2 itself.

First we evaluate the accuracy of \hat{p}_1 , the simple spherical cap volume approximate p value. We considered $m_0 = m_1$ in a range of values from 5 to 200. The values \hat{p}_1 ranged from just below 1 to 2×10^{-30} . We judge the accuracy of this estimate by its RMSE. Under distribution 1 this is $(\mathbb{E}(\hat{p}_1(\rho) - p(\mathbf{y}, \rho))^2)^{1/2}$ for $\mathbf{y} \sim \mathbf{U}(\mathbb{S}^d)$. Figure 4a shows this RMSE decreasing towards 0 as \hat{p}_1 goes to 0 with ρ going to 1. The RMSE also decreases with increasing sample size, as we would expect from the central limit theorem.

As seen in Figures 4a and 4b, the RMSE is not monotone in \hat{p}_1 . Right at $\hat{p}_1 = 1$ we know that RMSE = 0 and around 0.1 there is a dip. The practically interesting values of \hat{p}_1 are much smaller than 0.1, and the RMSE is monotone for them.

A problem with \hat{p}_1 is that it can approach 0 even though $p \geq 1/N$ must hold. The distribution 1 RMSE does not reflect this problem. By studying $\mathbb{E}_2((\hat{p}_1(\rho) - p(\mathbf{y}, \rho))^2)^{1/2}$, we get a different result. In Figure 4c, the RMSE of \hat{p}_1 under distribution 2 reaches a plateau as \hat{p}_1 goes to 0.

The estimator $\hat{p}_2 = \tilde{p}_0$ performs better than \hat{p}_1 because it makes more use of the data, and it is never below $1/N$. As seen in Figure 4d, the RMSE of \hat{p}_2 very closely matches \hat{p}_2 itself as \hat{p}_2 decreases to zero. That is, the relative error $|\hat{p}_2 - p|/\hat{p}_2$ is well behaved for small p -values. In rare event estimation, that property is known as strong efficiency (Blanchet and Glynn, 2008) and can be very hard to achieve. Here as \hat{p}_2 decreases to the granularity limit $1/N$, its RMSE actually decreases to 0. Eventually the distance from \mathbf{y}_0 to \mathbf{x}_0 is below the minimum interpoint distance among the \mathbf{x}_k and then, for a one-sided test, $\hat{p}_2 = p = 1/N$.

The estimators \hat{p}_1 and \hat{p}_2 , do not differ much for larger p -values as seen in Figure 5a. But in the limit as $\hat{p} \rightarrow 1$ we see that $\hat{p}_1 \rightarrow 0$, while \hat{p}_2 approaches the granularity limit $1/N$ instead.

Figure 5b compares the RMSE of the two estimators under distribution 2. As expected, \hat{p}_2 is more accurate. It also shows that the biggest differences occur only when \hat{p}_1 goes below $1/N$.

To examine the behavior of \hat{p}_2 more closely, we plot its coefficient of variation in Figure 6. We see that the relative uncertainty in \hat{p}_2 is not extremely large. Even when the estimated p -values are as small as 10^{-30} the coefficient of variation is below 5.

In Section 4, we mentioned another choice for \mathbf{x}_c . It was $\hat{p}_3 = \tilde{p}_c$, where \mathbf{x}_c is the closest permutation of \mathbf{x}_0 to \mathbf{y}_0 . Figure 2.7 in He (2016) compares \hat{p}_3 to \hat{p}_2 in some simulations. As expected, \hat{p}_3 tends to be larger (more conservative) than \hat{p}_2 , though it does sometimes come out smaller. Figure 2.8 of He (2016) compares the RMSE of \hat{p}_3 to \hat{p}_2 . The upward bias of \hat{p}_3 gave it a much larger RMSE.

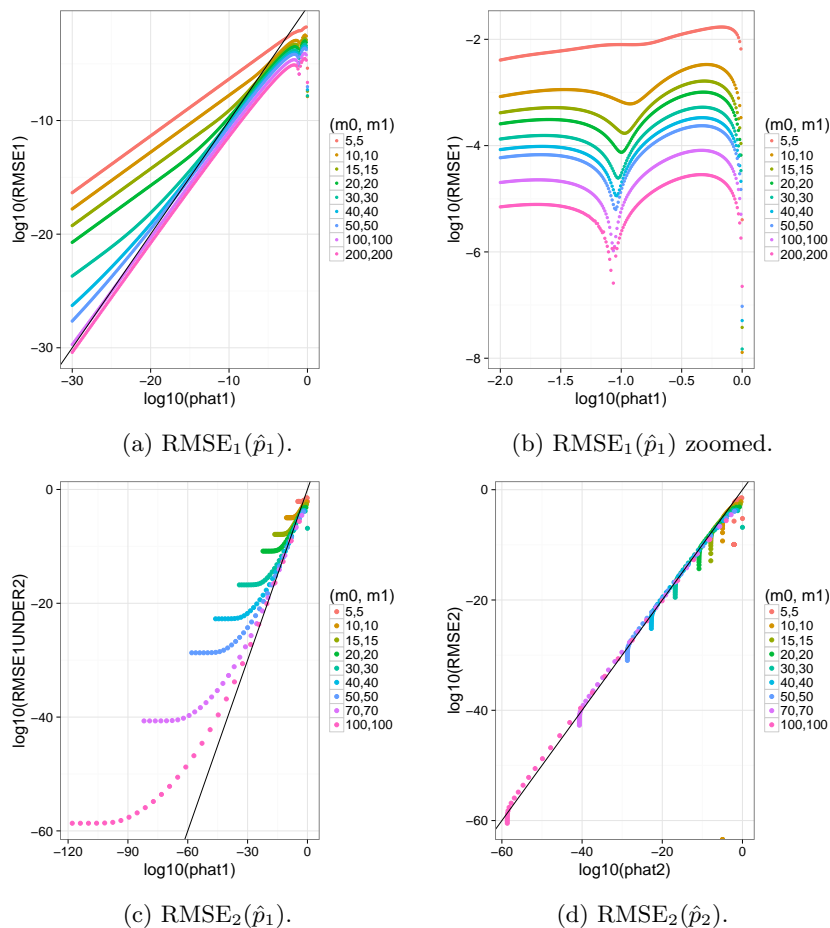


Fig 4: RMSEs for \hat{p}_1 and \hat{p}_2 under reference distributions 1 and 2. The x -axis shows the estimate \hat{p} as ρ varies from 1 to 0. Here $m_0 = m_1$. Plots with $m_0 \neq m_1$ are similar.

8. Comparison to saddlepoint approximation

The small relative error property of \hat{p}_2 is similar to the relative error property in saddlepoint approximations. Reid (1988) surveys saddlepoint approximations and Robinson (1982) develops them for permutation tests of the linear statistics we have considered here. When the true p -value is p , the saddlepoint approximation \hat{p}_s satisfies $\hat{p}_s = p(1 + O(1/n))$. Because we do not know the implied constant in $O(1/n)$ or the n at which it takes effect, the saddlepoint approximation does not provide a computable upper bound for the true permutation p -value p .

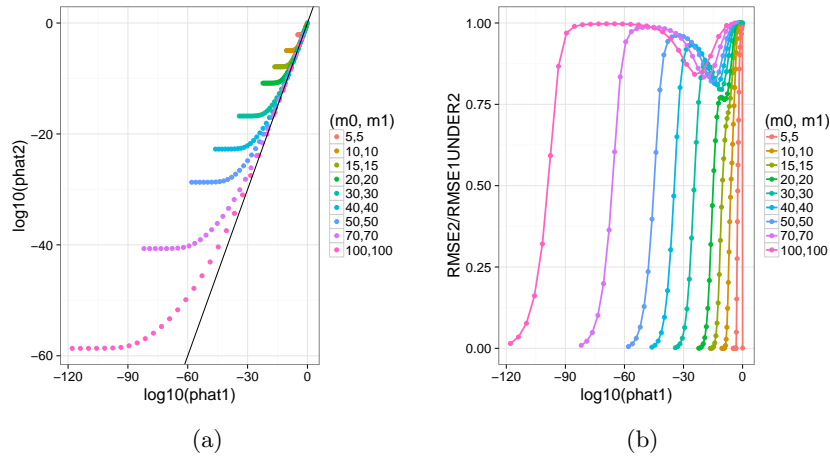


Fig 5: Comparison of \hat{p}_1 and \hat{p}_2 . In (a), $\log_{10}(\hat{p}_2)$ is plotted against $\log_{10}(\hat{p}_1)$ for varying ρ 's. The black line is the 45 degree line. In (b), the ratio of RMSEs for \hat{p}_1 and \hat{p}_2 is plotted against $\log_{10}(\hat{p}_1)$. The x -axis is $\log_{10}(\hat{p}_1)$.

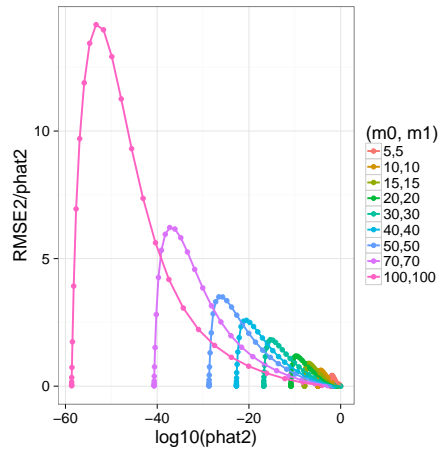


Fig 6: The coefficient of variation for \hat{p}_2 with varying ρ 's.

Figure 7 compares our estimates to each other and those of the saddlepoint approximation, equation (1) from Robinson (1982). The simulated data have the $\text{Exp}(1)$ distribution under the control condition and the $2 + \text{Exp}(1)$ distribution under the affected condition. The sample sizes were $m_0 = m_1 = 10$ making it feasible to compute the exact permutation p -value for hundreds of examples. In each case we ran 500 independent simulations. Cases with perfect separation were excluded: the saddlepoint approximation is numerically unstable then, and

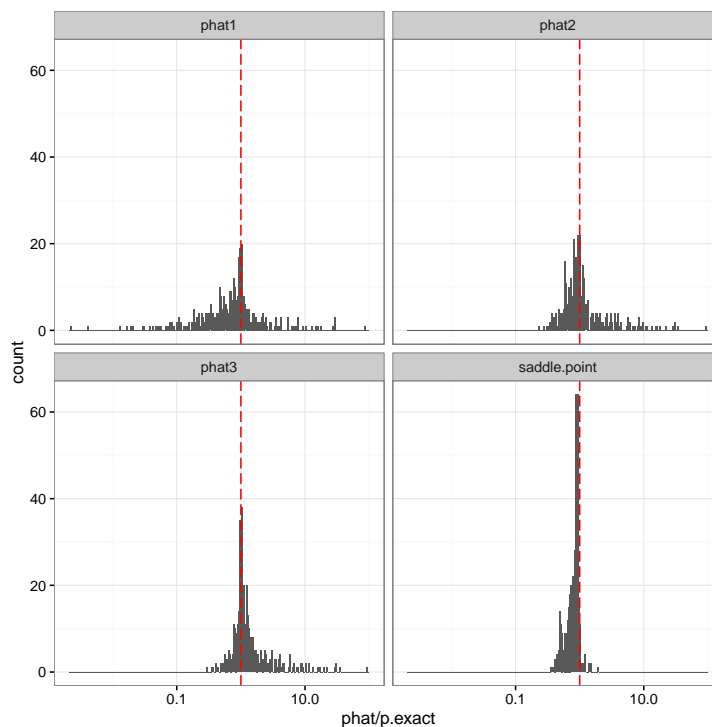


Fig 7: Simulation results \hat{p}/p as described in the text, for $Y_{0,i} \stackrel{\text{iid}}{\sim} \text{Exp}(1)$, and $Y_{1,i} \stackrel{\text{iid}}{\sim} \text{Exp}(1) + 2$.

one can easily detect that the minimum Y value in one group is larger than the maximum in the other group, showing that $p = 1/N$. In every instance we compared two-sided p -values. Chapter 2 of He (2016) considers simulations from some other distributions. The control condition data are $t_{(5)}$, $\mathcal{N}(0, 1)$ and $\mathbf{U}(0, 1)$ while the affected condition data are shifted versions of these distributions.

In these simulations, the naive spherical cap estimator \hat{p}_1 , with no good relative error properties, is consistently least accurate and is often much smaller than the true p . The saddlepoint estimate is very accurate but tends to come out smaller than the true p . The estimators \hat{p}_2 and \hat{p}_3 are less likely to be below p than the saddlepoint estimate, and by construction, they are never below the granularity limit. Qualitatively similar results happened for all of the distributions. The accuracy of all of these p -value estimates tends to be better for lighter tailed Y_i .

We can also construct Z scores, $Z_2 = (p - \hat{p}_2)/\text{RMSE}_2$ and a similar Z_3 . If these take large values, then it means that \hat{p} is too small and, moreover, that our computed RMSE does not diagnose it. The largest Z scores we observed are in Table 1. The largest Z values arose for exponential data with $p \doteq 0.89$ and

Dist'n $Y_{0,i}$	$\max Z_2$	$\max\{Z_2 \mid \hat{p}_2 < 0.1\}$	$\max Z_3$	$\max\{Z_3 \mid \hat{p}_3 < 0.1\}$
$t_{(5)}$	26.7	1.91	31.5	3.87
Exp(1)	7.55	7.55	7.76	7.76
$\mathbf{U}(0, 1)$	3.49	2.45	5.87	2.61
$\mathcal{N}(0, 1)$	3.07	2.78	3.07	2.78

TABLE 1

Maximal Z scores observed for \hat{p}_2 and \hat{p}_3 in 500 independent replications.

First author	m_1	m_0	$N = \binom{m_1+m_0}{m_1}$
Zhang	11	18	3.5×10^7
Moran	29	14	7.9×10^{10}
Scherzer	50	22	1.8×10^{18}

TABLE 2

Sample sizes for three microarray studies.

$\hat{p}_2 \doteq 0.78 \doteq \hat{p}_3$. Such large p -values are not very important and so maximal Z scores are also shown among estimated p -values below 0.1.

What we find is that the Z values are not very extreme. This suggests that it might be feasible to get a conservative p -value estimate by adding some multiple of the distribution 2 RMSE to \hat{p}_2 .

9. Data comparisons

Three data sets on Parkinson's disease were used by [Larson and Owen \(2015\)](#) and investigated in Chapter 6 of [He \(2016\)](#). They come from [Scherzer et al. \(2007\)](#), [Moran et al. \(2006\)](#) and [Zhang et al. \(2005\)](#). Table 2 shows their sample sizes.

For this comparison, there were 6180 gene sets from v5.1 of mSigDB's gene set collections. Curated gene sets and Gene Ontology gene sets were used. The gene sets ranged in size from 5 to 2131 genes with an average size of 93.08 genes. Slightly different versions of the gene sets were used in [Larson and Owen \(2015\)](#).

Ground truth estimates of two-sided p values for linear test statistics were obtained using $M = 10^6$ permutations. When the estimate was below 10^{-4} , the number M was increased to 10^7 . The Zhang data set had the smallest sample size and had no gene sets significant at below 0.01 and so we do not compare estimates for this gene set.

Table 3 gives correlations between \log_{10} estimated and gold-standard p -values for these genes. From Table 3, we see that \hat{p}_1 , \hat{p}_2 and \hat{p}_3 have nearly the same correlations with the gold standard; indeed they correlate highly with each other. They correlate with the gold standard estimate much more closely than the saddlepoint estimator does. Figures in Chapter 6 of [He \(2016\)](#) give scatterplots. These show the saddlepoint estimator is biased low and \hat{p}_3 is biased slightly high. Statistics \hat{p}_1 and \hat{p}_2 are quite close, possibly because none of the gene sets has a very small p -value.

While saddlepoint methods have a very desirable relative error property they do have some numerical issues. Table 4 shows some timing data. We also got in-

Data	Correlation	\hat{p}_1	\hat{p}_2	\hat{p}_3	\hat{p}_{saddle}
Moran	Pearson	0.9997	0.9997	0.9997	0.9937
	Kendall	0.9856	0.9856	0.9866	0.9395
Scherzer	Pearson	0.9997	0.9997	0.9997	0.9837
	Kendall	0.9869	0.9869	0.9870	0.8937
Moran Low	Pearson	0.9501	0.9504	0.9653	0.7125
Moran Low	Kendall	0.8283	0.8283	0.8578	0.5411
Scherzer Low	Pearson	0.9940	0.9940	0.9947	0.8652
Scherzer Low	Kendall	0.9429	0.9429	0.9429	0.7714

TABLE 3

The table gives both Pearson and Kendall correlations over 6180 gene sets, between estimated $\log_{10}(p)$ -values and gold standard $\log_{10}(p)$ -values for both the Moran and Scherzer data sets. The designation ‘Low’ refers to only the 190 gene sets with p -values in the interval $(10^{-5}, 10^{-4})$ for Moran, or the 15 gene sets with p -values in the interval $(10^{-5}, 10^{-3})$ for Scherzer.

Data Set	Saddle	\hat{p}_1	\hat{p}_2	\hat{p}_3
Zhang	0.0631	0.0024	0.0031	0.0032
Moran	0.0894	0.0029	0.0037	0.0038
Scherzer	0.1394	0.0034	0.0045	0.0047

TABLE 4

Average, over 6180 gene sets of the running time in seconds for saddlepoint p -values and \hat{p}_j , $j = 1, 2, 3$. Total time ranges from under 1/4 minute to just over 14 minutes.

finite values for 95 of the gene sets on the Zhang data. It might be a convergence issue or possibly a flaw in how we implemented saddlepoints.

10. Discussion

We have constructed approximations to the permutation p -value using probability and geometry derived from discrepancy theory. A rigorous upper bound for p could be attained using L_∞ spherical cap discrepancies instead of the L_2 version, but computing such discrepancies is a major challenge. [Narcowich et al. \(2010\)](#) give upper bounds for the L_∞ spherical cap discrepancy, in terms of averages of a great many harmonic functions at the points \mathbf{x}_i . For our application we need bounds for spherical caps of a fixed volume (under distribution 1) and of fixed volume and constrained location (under distribution 2) and those go beyond what is in [Narcowich et al. \(2010\)](#).

Many other approximation methods have been proposed for permutation tests. For instance, [Zhou et al. \(2009\)](#) fit approximations by moments in the Pearson family. [Larson and Owen \(2015\)](#) fit Gaussian and beta approximations to linear statistics and gamma approximations to quadratic statistics for gene set testing problems. [Knijnenburg et al. \(2009\)](#) fit generalized extreme value distributions to the tails of sampled permutation values.

None of these approximations come with an all inclusive p -value that accounts for both numerical uncertainty of the estimation and sampling uncer-

tainty behind the original data. IID sampling of permutations does come with such a p -value if we add one to numerator and denominator as [Barnard \(1963\)](#) suggests. Then the Monte Carlo p -value estimate \hat{p} is actually a conservative p -value in it's own right: $\Pr(\hat{p} \leq u) \leq u$ for $0 \leq u \leq 1$ under the null hypothesis. However, that method cannot attain very small p -values, and so a gap remains.

We have employed reference distributions in an effort to address this gap. We select a set \mathbb{Y} containing \mathbf{y}_0 and find the first two moments of $p(\mathbf{y}, \hat{\rho})$ for $\mathbf{y} \sim \mathbf{U}(\mathbb{Y})$. If the data \mathbf{y}_0 were actually sampled from our reference distribution, then we could get an all inclusive conservative p -value via the Chebychev inequality.

To illustrate the Chebychev inequality, let $\mu = \mathbb{E}(p(\mathbf{y}, \hat{\rho}))$ and $\sigma^2 = \text{Var}(p(\mathbf{y}, \hat{\rho}))$ for the observed value $\hat{\rho} = \mathbf{x}_0^\top \mathbf{y}_0$ and for random $\mathbf{y} \sim \mathbf{U}(\mathbb{Y})$ for some reference set \mathbb{Y} . Then $\Pr(p \geq \mu + \lambda\sigma) \leq 1/(1 + \lambda^2)$ for any $\lambda > 0$. Under this model, $p^* = \mu + \lambda\sigma + 1/(1 + \lambda^2)$ is a conservative p -value. Minimizing p^* over λ reduces to solving $2\lambda = \sigma(1 + \lambda^2)^2$. For small p we anticipate $\lambda \gg 1$ and hence $\lambda' = (2/\sigma)^{1/3}$ will be almost as good as the optimal λ we could find numerically. That choice leads to $p^* \leq \mu + (2^{1/3} + 2^{-2/3})\sigma^{2/3}$.

For a numerical illustration, consider $\mu = 10^{-30}$ and $\sigma = 3 \times 10^{-30}$, roughly describing the small p -value estimates from the case $m_0 = m_1 = 70$. Then $p^* \leq 4 \times 10^{-20}$, much larger than μ and yet still very small, likely small enough to be significant after multiplicity adjustments.

The reference distributions describe a set in which $p(\mathbf{y}_0, \hat{\rho})$ is known to lie. Reference distribution 1 applies for Gaussian Y_i and reference distribution 2 is for Gaussian Y_i after conditioning on $\mathbf{y}^\top \mathbf{x}_0 = \mathbf{y}_0^\top \mathbf{x}_0$. Of course, the data will not ordinarily be exactly Gaussian. The numerical illustration uses a Chebychev inequality at $\lambda' \doteq 8.7 \times 10^9$ standard deviations.

As mentioned above, an L_∞ version of the Stolarsky inequality would eliminate the need for Chebychev inequalities though it might also be very conservative. We do not know whether $p(\mathbf{y}, \hat{\rho})$ has a heavy tailed distribution under reference distribution 2.

Our permutation points fall into a lattice subset of \mathbb{R}^d intersected with the unit sphere \mathbb{S}^d . Our problem of counting the number of such points in a subset is one that is addressed under the term 'Geometry of numbers'. According to a personal communication from Neil Sloane, the standard approach to such problems is via the volume ratio, which in our setting is \hat{p}_1 which does not do well for our problems.

To have reasonable power to obtain a p -value below ϵ by permutation sampling requires on the order of $1/\epsilon$ permutations each requiring $O(n \log(n))$ computation to generate and $O(n)$ computation to evaluate the inner product. The cost to compute the standard errors in our method is dominated by a cost proportional to \underline{m}^3 though there is a very small cost proportional to \underline{m}^4 . In the range where the first cost dominates, our proposal is advantageous when $\underline{m}^3 = o(n/\epsilon)$. Supposing that m_0 and m_1 are comparable, our advantage holds when $\underline{m}^2 = o(1/\epsilon)$. If only the estimate and not the standard error is required, then our \hat{p}_2 and \hat{p}_3 cost $O(\underline{m})$ once the $\hat{\rho}$ (cost $O(n)$) has been computed. Then the total cost is $O(n)$ compared to the much larger cost $O(n/\epsilon)$ for sampling.

Acknowledgements

This work was supported by the US National Science Foundation under grants DMS-1407397 and DMS-1521145. We thank John Robinson and Neil Sloane for helpful comments.

References

- Ackermann, M. and Strimmer, K. (2009). A general modular framework for gene set enrichment analysis. *BMC Bioinformatics*, 10:1–20.
- Aronszajn, N. (1950). Theory of reproducing kernels. *Transactions of the American Mathematical Society*, 68(3):337–404.
- Barnard, G. A. (1963). Discussion of the spectral analysis of point processes (by m. s. bartlett). *Journal of the Royal Statistical Society, series B*, 25:294.
- Bilyk, D., Dai, F., and Matzke, R. (2016). Stolarsky principle and energy optimization on the sphere. Technical report.
- Blanchet, J. and Glynn, P. (2008). Efficient rare-event simulation for the maximum of heavy-tailed random walks. *The Annals of Applied Probability*, pages 1351–1378.
- Brauchart, J. and Dick, J. (2013). A simple proof of Stolarsky’s invariance principle. *Proceedings of the American Mathematical Society*, 141(6):2085–2096.
- Fadista, J., Manning, A. K., Florez, J. C., and Groop, L. (2016). The (in) famous GWAS p-value threshold revisited and updated for low-frequency variants. *European Journal of Human Genetics*, 24(8):1202–1205.
- He, H. (2016). *Efficient Permutation-Based P-Value Estimation for Gene Set Tests*. PhD thesis, Stanford University.
- Jiang, Z. and Gentleman, R. (2007). Extensions to gene set enrichment. *Bioinformatics*, 23(3):306–313.
- Knijnenburg, T. A., Wessels, L. F. A., Reinders, M. J. T., and Shmulevich, I. (2009). Fewer permutations, more accurate p-values. *Bioinformatics*, 25(12):i161–i168.
- Larson, J. L. and Owen, A. B. (2015). Moment based gene set tests. *BMC Bioinformatics*, 16(1):132.
- Lee, Y. and Kim, W. C. (2014). Concise formulas for the surface area of the intersection of two hyperspherical caps. Technical report, Korea advanced institute of science and technology.
- Moran, L. B., Duke, D. C., Deprez, M., Dexter, D. T., Pearce, R. K. B., and Graeber, M. B. (2006). Whole genome expression profiling of the medial and lateral substantia nigra in parkinsons disease. *Neurogenetics*, 7(1):1–11.
- Narcowich, F. J., Sun, X., Ward, J. D., and Wu, Z. (2010). Leveque type inequalities and discrepancy estimates for minimal energy configurations on spheres. *Journal of Approximation Theory*, 162(6):1256–1278.
- Niederreiter, H. (1992). *Random Number Generation and Quasi-Monte Carlo Methods*. SIAM, Philadelphia, PA.

- Reid, N. (1988). Saddlepoint methods and statistical inference. *Statistical Science*, pages 213–227.
- Robinson, J. (1982). Saddlepoint approximations for permutation tests and confidence intervals. *Journal of the Royal statistical society, Series B*, pages 91–101.
- Scherzer, C. R., AC, A. C. E., Morse, L. J., Liao, Z., Locascio, J. J., Fefer, D., Schwarzschild, M. A., Schlossmacher, M. G., Hauser, M. A., Vance, J. M., Sudarsky, L. R., Standaert, D. G., Growdon, J. H., Jensen, R. V., and Gullans, S. R. (2007). Molecular markers of early Parkinson’s disease based on gene expression in blood. *Proc Natl Acad Sci*, 104(3):955–60.
- Stolarsky, K. B. (1973). Sums of distances between points on a sphere. II. *Proceedings of the American Mathematical Society*, 41(2):575–582.
- Zhang, Y., James, M., Middleton, F. A., and Davis, R. L. (2005). Transcriptional analysis of multiple brain regions in Parkinson’s disease supports the involvement of specific protein processing, energy metabolism, and signaling pathways, and suggests novel disease mechanisms. *American J Med Genet B Neuropsychiatry Genet*, 137B(1):5–16.
- Zhou, C., Wang, H. J., and Wang, Y. M. (2009). Efficient moments-based permutation tests. In *Advances in neural information processing systems*, pages 2277–2285.

11. Appendix

Here we collect up some of the longer proofs.

11.1. Proof of Theorem 3 (Limiting invariance)

Here we show that taking limits as ϵ goes to zero in the formula of [Brauchart and Dick \(2013\)](#) proves Theorem 3. We use three lemmas, one for each term in Theorem 2. We use $\epsilon \rightarrow 0$ as a shorthand for $\lim_{\epsilon_1 \rightarrow 0^+} \lim_{\epsilon_2 \rightarrow 0^+}$.

Lemma 4. *Let v_ϵ be defined as in (3.3). Then for $\hat{\rho} \in [-1, 1)$,*

$$\begin{aligned} & \lim_{\epsilon \rightarrow 0} \int_{-1}^1 v_\epsilon(t) \int_{\mathbb{S}^d} \left| \sigma_d(C(\mathbf{z}; t)) - \frac{1}{N} \sum_{k=0}^{N-1} \mathbf{1}_{C(\mathbf{z}; t)}(\mathbf{x}_k) \right|^2 d\sigma_d(\mathbf{z}) dt \\ &= \int_{\mathbb{S}^d} |p(\mathbf{z}, \hat{\rho}) - \hat{p}(\hat{\rho})|^2 d\sigma_d(\mathbf{z}). \end{aligned}$$

Proof. Substituting v_ϵ we get

$$\begin{aligned} & \int_{-1}^1 \left(\epsilon_2 + \frac{1}{\epsilon_1} \mathbf{1}(\hat{\rho} \leq t \leq \hat{\rho} + \epsilon_1) \right) \int_{\mathbb{S}^d} (\hat{p}(t) - p(\mathbf{z}, t))^2 d\sigma_d(\mathbf{z}) dt \\ \rightarrow & \frac{1}{\epsilon_1} \int_{\hat{\rho}}^{\hat{\rho} + \epsilon_1} \int_{\mathbb{S}^d} (\hat{p}(t) - p(\mathbf{z}, t))^2 d\sigma_d(\mathbf{z}) dt, \quad \text{as } \epsilon_2 \rightarrow 0^+ \\ \rightarrow & \int_{\mathbb{S}^d} (\hat{p}(\hat{\rho}) - p(\mathbf{z}, \hat{\rho}))^2 d\sigma_d(\mathbf{z}), \quad \text{as } \epsilon_1 \rightarrow 0^+. \quad \square \end{aligned}$$

Lemma 5. Let v_ϵ be as in (3.3) with $\hat{\rho} \in [-1, 1)$, and let K_{v_ϵ} be given by (3.2). Then for any $\mathbf{x}, \mathbf{x}' \in \mathbb{S}^d$,

$$\lim_{\epsilon \rightarrow 0} K_{v_\epsilon}(\mathbf{x}, \mathbf{x}') = \sigma_d(C(\mathbf{x}; \hat{\rho}) \cap C(\mathbf{x}'; \hat{\rho})).$$

Proof. The argument is essentially the same as for Lemma 4. \square

Lemma 6. Let v_ϵ be as in (3.3) with $\hat{\rho} \in [-1, 1)$, and let K_{v_ϵ} be given by (3.2). Then

$$\lim_{\epsilon \rightarrow 0} \int_{\mathbb{S}^d} \int_{\mathbb{S}^d} K_{v_\epsilon}(\mathbf{x}, \mathbf{y}) d\sigma_d(\mathbf{x}) d\sigma_d(\mathbf{y}) = \hat{p}_1(\hat{\rho})^2. \quad (11.1)$$

Proof. For any $\mathbf{x}, \mathbf{y} \in \mathbb{S}^d$, the kernel $K_{v_\epsilon}(\mathbf{x}, \mathbf{y})$ is nonnegative and upper bounded by a constant. Therefore we can take our limit operations inside the double integral over \mathbf{x} and \mathbf{y} . Now $\lim_{\epsilon \rightarrow 0} K_{v_\epsilon}(\mathbf{x}, \mathbf{y}) = \int_{\mathbb{S}^d} \mathbf{1}_{C(\mathbf{z}; \hat{\rho})}(\mathbf{x}) \mathbf{1}_{C(\mathbf{z}; \hat{\rho})}(\mathbf{y}) d\sigma_d(\mathbf{z})$. Therefore the limit in (11.1) is

$$\int_{\mathbb{S}^d} \int_{\mathbb{S}^d} \int_{\mathbb{S}^d} \mathbf{1}_{C(\mathbf{z}; \hat{\rho})}(\mathbf{x}) \mathbf{1}_{C(\mathbf{z}; \hat{\rho})}(\mathbf{y}) d\sigma_d(\mathbf{z}) d\sigma_d(\mathbf{y}) d\sigma_d(\mathbf{x}) = \hat{p}_1(\hat{\rho})^2$$

after changing the order of the integrals. \square

Theorem 3 Let $\mathbf{x}_0, \mathbf{x}_1, \dots, \mathbf{x}_N \in \mathbb{S}^d$ and $\hat{\rho} \in [-1, 1]$. Then

$$\int_{\mathbb{S}^d} |p(\mathbf{z}, \hat{\rho}) - \hat{p}_1(\hat{\rho})|^2 d\sigma_d(\mathbf{z}) = \frac{1}{N^2} \sum_{k=0}^{N-1} \sum_{l=0}^{N-1} \sigma_d(C(\mathbf{x}_k; \hat{\rho}) \cap C(\mathbf{x}_l; \hat{\rho})) - \hat{p}_1(\hat{\rho})^2.$$

Proof. Theorem 2 gives us an identity and applying Lemmas 4, 5 and 6 to both sides of it establishes (3.4) for $\rho \in [-1, 1)$. For $\hat{\rho} = 1$ we get the answer by replacing v_ϵ by $\epsilon_2 + (1/\epsilon_1) \mathbf{1}_{1-\epsilon_1 \leq t \leq 1}$ in the lemmas. Replacing \mathbf{z} by \mathbf{y} and $\hat{\rho}$ by t above gives the version in the main body of the article. \square

11.2. Proof of Lemma 3 (Double inclusion for Model 2)

Proof. We split the proof into four cases and prove them individually. Recall that $P_2(u_1, u_2, u_3, \tilde{\rho}, \hat{\rho}) = \int_{\mathbb{S}^{d-1}} \mathbf{1}(\langle \mathbf{y}, \mathbf{x}_1 \rangle \geq \tilde{\rho}) \mathbf{1}(\langle \mathbf{y}, \mathbf{x}_2 \rangle \geq \hat{\rho}) d\sigma_{d-1}(\mathbf{y}^*)$ where $\mathbf{y} = \tilde{\rho} \mathbf{x}_c + \sqrt{1 - \tilde{\rho}^2} \mathbf{y}^*$.

Case 1. $\mathbf{x}_1 = \mathbf{x}_2 = \mathbf{x}_c$, i.e., $r_1 = r_2 = r_3 = 0$.

$$P_2(1, 1, 1, \tilde{\rho}, \hat{\rho}) = \int_{\mathbb{S}^{d-1}} \mathbf{1}(\langle \mathbf{y}, \mathbf{x}_c \rangle \geq \hat{\rho}) \mathbf{1}(\langle \mathbf{y}, \mathbf{x}_c \rangle \geq \tilde{\rho}) d\sigma_{d-1}(\mathbf{y}^*) = \mathbf{1}(\tilde{\rho} \geq \hat{\rho}).$$

Case 2. $\mathbf{x}_1 = \mathbf{x}_c \neq \mathbf{x}_2$, i.e., $r_1 = 0, r_2 > 0, r_3 > 0$.

$$\begin{aligned} P_2(1, u_2, u_2, \tilde{\rho}, \hat{\rho}) &= \int_{\mathbb{S}^{d-1}} \mathbf{1}(\langle \mathbf{y}, \mathbf{x}_c \rangle \geq \hat{\rho}) \mathbf{1}(\langle \mathbf{y}, \mathbf{x}_2 \rangle \geq \tilde{\rho}) d\sigma_{d-1}(\mathbf{y}^*) \\ &= \mathbf{1}(\tilde{\rho} \geq \hat{\rho}) \int_{\mathbb{S}^{d-1}} \mathbf{1}(\langle \mathbf{y}, \mathbf{x}_2 \rangle \geq \tilde{\rho}) d\sigma_{d-1}(\mathbf{y}^*) \\ &= \mathbf{1}(\tilde{\rho} \geq \hat{\rho}) P_1(u_2, \tilde{\rho}, \hat{\rho}) \end{aligned}$$

where the last step uses Lemma 2.

Case 3. $\mathbf{x}_1 = \mathbf{x}_2 \neq \mathbf{x}_c$, i.e., $r_1 = r_2 > 0 = r_3$.

$$\begin{aligned} P_2(u_2, u_2, 1, \tilde{\rho}, \hat{\rho}) &= \int_{\mathbb{S}^{d-1}} \mathbf{1}(\langle \mathbf{y}, \mathbf{x}_1 \rangle \geq \hat{\rho}) \mathbf{1}(\langle \mathbf{y}, \mathbf{x}_2 \rangle \geq \tilde{\rho}) d\sigma_{d-1}(\mathbf{y}^*) \\ &= \int_{\mathbb{S}^{d-1}} \mathbf{1}(\langle \mathbf{y}, \mathbf{x}_2 \rangle \geq \tilde{\rho}) d\sigma_{d-1}(\mathbf{y}^*) \\ &= P_1(u_2, \tilde{\rho}, \hat{\rho}). \end{aligned}$$

Case 4. $\mathbf{x}_1 \neq \mathbf{x}_2 \neq \mathbf{x}_c \neq \mathbf{x}_1$, i.e., $r_1, r_2, r_3 > 0$. We split this case into subcases. First we assume $u_2 = -1$, so

$$\begin{aligned} P_2(u_1, u_2, u_3, \tilde{\rho}, \hat{\rho}) &= \int_{\mathbb{S}^{d-1}} \mathbf{1}(\langle \mathbf{y}, \mathbf{x}_1 \rangle \geq \hat{\rho}) \mathbf{1}(\langle \mathbf{y}, -\mathbf{x}_c \rangle \geq \tilde{\rho}) d\sigma_{d-1}(\mathbf{y}^*) \\ &= \mathbf{1}(-\tilde{\rho} \geq \hat{\rho}) \int_{\mathbb{S}^{d-1}} \mathbf{1}(\langle \mathbf{y}, \mathbf{x}_1 \rangle \geq \hat{\rho}) d\sigma_{d-1}(\mathbf{y}^*) \\ &= \mathbf{1}(-\tilde{\rho} \geq \hat{\rho}) P_1(u_1, \tilde{\rho}, \hat{\rho}). \end{aligned}$$

Similarly if $u_1 = -1$, then

$$P_2(u_1, u_2, u_3, \tilde{\rho}, \hat{\rho}) = \mathbf{1}(-\tilde{\rho} \geq \hat{\rho}) P_1(u_2, \tilde{\rho}, \hat{\rho}).$$

Finally we assume $u_1 > -1$ and $u_2 > -1$, so now $|u_1| < 1$ and $|u_2| < 1$. Recall the projections $\mathbf{x}_j = u_j \mathbf{c}_c + \sqrt{1 - u_j^2} \mathbf{x}_j^*$ for $j = 1, 2$ and introduce further projections of \mathbf{y}^* and \mathbf{x}_2^* onto \mathbf{x}_1^* : $\mathbf{y}^* = t \mathbf{x}_1^* + \sqrt{1 - t^2} \mathbf{y}^{**}$ and $\mathbf{x}_2^* = u_3^* \mathbf{x}_1^* + \sqrt{1 - u_3^{*2}} \mathbf{x}_2^{**}$. The residuals \mathbf{y}^{**} and \mathbf{x}_2^{**} belong to a subset of \mathbb{S}^d that is

isomorphic to \mathbb{S}^{d-2} . Now we have

$$\begin{aligned}
& P_2(u_1, u_2, u_3, \tilde{\rho}, \hat{\rho}) \\
&= \int_{\mathbb{S}^{d-1}} \mathbf{1}(\langle \mathbf{y}, \mathbf{x}_1 \rangle \geq \hat{\rho}) \mathbf{1}(\langle \mathbf{y}, \mathbf{x}_2 \rangle \geq \tilde{\rho}) d\sigma_{d-1}(\mathbf{y}^*) \\
&= \int_{-1}^1 \frac{\omega_{d-2}}{\omega_{d-1}} (1-t^2)^{\frac{d-1}{2}-1} \int_{\mathbb{S}^{d-2}} \mathbf{1}(\tilde{\rho}u_1 + \sqrt{1-\tilde{\rho}^2}\sqrt{1-u_1^2}t \geq \hat{\rho}) \\
&\quad \times \mathbf{1}(\tilde{\rho}u_2 + \sqrt{1-\tilde{\rho}^2}\sqrt{1-u_2^2}(tu_3^* + \sqrt{1-t^2}\sqrt{1-u_3^{*2}}\langle \mathbf{y}^{**}, \mathbf{x}_2^{**} \rangle) \geq \hat{\rho}) \\
&\quad \times d\sigma_{d-1}(\mathbf{y}^{**}) dt \\
&= \int_{-1}^1 \frac{\omega_{d-2}}{\omega_{d-1}} (1-t^2)^{\frac{d-1}{2}-1} \mathbf{1}\left(t \geq \frac{\hat{\rho} - \tilde{\rho}u_1}{\sqrt{1-\tilde{\rho}^2}\sqrt{1-u_1^2}}\right) \\
&\quad \times \int_{\mathbb{S}^{d-2}} \mathbf{1}(\tilde{\rho}u_2 + \sqrt{1-\tilde{\rho}^2}\sqrt{1-u_2^2}(tu_3^* + \sqrt{1-t^2}\sqrt{1-u_3^{*2}}\langle \mathbf{y}^{**}, \mathbf{x}_2^{**} \rangle) \geq \hat{\rho}) \\
&\quad \times d\sigma_{d-1}(\mathbf{y}^{**}) dt \\
&= \begin{cases} \mathbf{1}(\tilde{\rho}u_1 \geq \hat{\rho})\mathbf{1}(\tilde{\rho}u_2 \geq \hat{\rho}), & \tilde{\rho} = \pm 1 \\ \int_{-1}^1 \frac{\omega_{d-2}}{\omega_{d-1}} (1-t^2)^{\frac{d-1}{2}-1} \mathbf{1}(t \geq \rho_1)\mathbf{1}(tu_3^* \geq \rho_2) dt, & \tilde{\rho} \neq \pm 1, u_3^* = \pm 1 \\ \int_{-1}^1 \frac{\omega_{d-2}}{\omega_{d-1}} (1-t^2)^{\frac{d-1}{2}-1} \mathbf{1}(t \geq \rho_1)\sigma_{d-2}\left(C(\mathbf{x}_2^{**}, \frac{\rho_2 - tu_3^*}{\sqrt{1-t^2}\sqrt{1-u_3^{*2}}})\right) dt, & \tilde{\rho} \neq \pm 1, |u_3^*| < 1 \end{cases}
\end{aligned}$$

where u_3^*, ρ_1, ρ_2 are defined in (4.7). Hence, the result follows. \square

11.3. Proof of Theorem 6 (Second moment under reference distribution 2)

Proof. Without loss of generality we relabel the values \mathbf{x}_k so that $c = 0$. Any other choice for c is reflected in the number $\tilde{\rho}$. The second moment is

$$\mathbb{E}(p(\mathbf{y}, \hat{\rho})^2) = \frac{1}{N^2} \sum_{k=0}^{N-1} \sum_{l=0}^{N-1} P_2(u_k, u_l, u_{k,\ell}, \tilde{\rho}, \hat{\rho}) \quad (11.2)$$

where $u_{k,\ell}$ is obtained via (2.1) from the swap distance $r_{k,\ell}$ between points \mathbf{x}_k and \mathbf{x}_ℓ . We will partition the sum in (11.2) into the same four cases as in the proof of Lemma 3.

Case 1, $\mathbf{x}_k = \mathbf{x}_\ell = \mathbf{x}_c$, i.e., $r_k = r_\ell = r_{k,\ell} = 0$. There is only one pair of $(\mathbf{x}_k, \mathbf{x}_\ell)$ for this condition. Hence, we get only one term corresponding to $P_2(1, 1, 1, \tilde{\rho}, \hat{\rho}) = \mathbf{1}(\tilde{\rho} \geq \hat{\rho})$.

Case 2, $\mathbf{x}_k = \mathbf{x}_c \neq \mathbf{x}_\ell$, i.e., $r_k = 0, r_\ell = r_{k,\ell} > 0$. Consider all pairs of $(\mathbf{x}_k, \mathbf{x}_\ell)$ that satisfy this condition and let K_2 denote their total contribution

to (11.2). Then

$$\begin{aligned} K_2 &= 2 \sum_{l=1}^{N-1} \int_{\mathbb{S}^{d-1}} \mathbf{1}(\langle \mathbf{y}, \mathbf{x}_c \rangle \geq \hat{\rho}) \mathbf{1}(\langle \mathbf{y}, \mathbf{x}_\ell \rangle \geq \hat{\rho}) d\sigma_{d-1}(\mathbf{y}^*) \\ &= 2 \sum_{r=1}^{\underline{m}} \binom{m_0}{r} \binom{m_1}{r} P_2(1, u(r), u(r), \tilde{\rho}, \hat{\rho}). \end{aligned}$$

Case 3, $\mathbf{x}_k = \mathbf{x}_\ell \neq \mathbf{x}_c$, i.e., $r_k = r_\ell > 0 = r_{k,\ell}$. The contribution from terms of this form is

$$K_3 = \sum_{k=1}^{N-1} \int_{\mathbb{S}^{d-1}} \mathbf{1}(\langle \mathbf{y}, \mathbf{x}_k \rangle \geq \hat{\rho}) d\sigma_{d-1}(\mathbf{y}^*) = \sum_{r=1}^{\underline{m}} \binom{m_0}{r} \binom{m_1}{r} P_1(u(r), \tilde{\rho}, \hat{\rho}).$$

Case 4, $\mathbf{x}_k \neq \mathbf{x}_\ell \neq \mathbf{x}_c$, i.e., $r_k, r_\ell, r_{k,\ell} > 0$. The contribution of these cases to the sum is

$$\begin{aligned} K_4 &= \sum_{k=1}^{N-1} \sum_{\ell=1}^{N-1} \mathbf{1}(\ell \neq k) \int_{\mathbb{S}^{d-1}} \mathbf{1}(\langle \mathbf{y}, \mathbf{x}_i \rangle \geq \hat{\rho}) \mathbf{1}(\langle \mathbf{y}, \mathbf{x}_j \rangle \geq \hat{\rho}) d\sigma_{d-1}(\mathbf{y}^*) \\ &= \sum_{r_k \in R} \sum_{r_\ell \in R} \sum_{r_{k,\ell} \in R_3(\mathbf{r})} c(r_k, r_\ell, r_{k,\ell}) P_2(u_1, u_2, u_3, \tilde{\rho}, \hat{\rho}). \end{aligned}$$

Then the second moment is $(\mathbf{1}(\tilde{\rho} \geq \hat{\rho}) + K_2 + K_3 + K_4)/N^2$. \square

11.4. Proof of Theorem 7 (Location weighted invariance)

Proof. We follow the technique in Brauchart and Dick (2013). We begin by showing that $K_{v,h,\mathbf{x}'}$ as defined in (5.2) is a reproducing kernel. First, $K_{v,h,\mathbf{x}'}$ is symmetric: $K_{v,h,\mathbf{x}'}(\mathbf{x}, \mathbf{y}) = K_{v,h,\mathbf{x}'}(\mathbf{y}, \mathbf{x})$. Next, choose $a_0, \dots, a_{N-1} \in \mathbb{R}$ and $\mathbf{x}_0, \dots, \mathbf{x}_{N-1} \in \mathbb{S}^d$. Then $\sum_{k,\ell=0}^{N-1} a_k a_\ell K_{v,h,\mathbf{x}'}(\mathbf{x}_k, \mathbf{x}_\ell)$ equals

$$\begin{aligned} & \int_{-1}^1 \int_{\mathbb{S}^d} \sum_{k,\ell=0}^{N-1} a_k a_\ell v(t) h(\langle \mathbf{z}, \mathbf{x}' \rangle) \mathbf{1}_{C(\mathbf{z};t)}(\mathbf{x}_k) \mathbf{1}_{C(\mathbf{z};t)}(\mathbf{x}_\ell) d\sigma_d(\mathbf{z}) dt \\ &= \int_{-1}^1 \int_{\mathbb{S}^d} v(t) h(\langle \mathbf{z}, \mathbf{x}' \rangle) \left| \sum_{k=0}^{N-1} a_k \mathbf{1}_{C(\mathbf{z};t)}(\mathbf{x}_k) \right|^2 d\sigma_d(\mathbf{z}) dt \end{aligned}$$

which is nonnegative. Thus $K_{v,h,\mathbf{x}'}$ is symmetric and positive definite, and so by Aronszajn (1950), $K_{v,h,\mathbf{x}'}$ is a reproducing kernel.

Aronszajn (1950) also shows that a reproducing kernel uniquely defines a Hilbert space of functions with a specific inner product. Let $\mathcal{H}_{v,h,\mathbf{x}'} = \mathcal{H}(K_{v,h,\mathbf{x}'}, \mathbb{S}^d)$ denote the corresponding reproducing kernel Hilbert space of functions $f: \mathbb{S}^d \rightarrow \mathbb{R}$ with reproducing kernel $K_{v,h,\mathbf{x}'}$.

We now consider functions $f_1, f_2 : \mathbb{S}^d \rightarrow \mathbb{R}$ which admit the representation

$$f_i(\mathbf{x}) = \int_{-1}^1 \int_{\mathbb{S}^d} g_i(\mathbf{z}; t) \mathbf{1}_{C(\mathbf{z}; t)}(\mathbf{x}) d\sigma_d(\mathbf{z}) dt, \quad i = 1, 2 \quad (11.3)$$

for functions $g_i \in L_2(\mathbb{S}^d \times [-1, 1])$. For any fixed $\mathbf{y} \in \mathbb{S}^d$ the function $K_{v, h, \mathbf{x}'}(\cdot, \mathbf{y})$ has representation (11.3) via $g(\mathbf{z}; t) = v(t)h(\langle \mathbf{z}, \mathbf{x}' \rangle) \mathbf{1}_{C(\mathbf{z}; t)}(\mathbf{y})$.

For functions with representation (11.3), we define an inner product by

$$\langle f_1, f_2 \rangle_{K_{v, h, \mathbf{x}'}} = \int_{-1}^1 \frac{1}{v(t)} \int_{\mathbb{S}^d} \frac{1}{h(\langle \mathbf{z}, \mathbf{x}' \rangle)} g_1(\mathbf{z}, t) g_2(\mathbf{z}, t) d\sigma_d(\mathbf{z}) dt. \quad (11.4)$$

For $\mathbf{y} \in \mathbb{S}^d$ and $f_1 \in \mathcal{H}_{v, h, \mathbf{x}'}$,

$$\begin{aligned} \langle f_1, K_{v, h, \mathbf{x}'}(\cdot, \mathbf{y}) \rangle_{K_{v, h, \mathbf{x}'}} &= \int_{-1}^1 \frac{1}{v(t)} \int_{\mathbb{S}^d} \frac{g_1(\mathbf{z}; t)v(t)}{h(\langle \mathbf{z}, \mathbf{x}' \rangle)} h(\langle \mathbf{z}, \mathbf{x}' \rangle) \mathbf{1}_{C(\mathbf{z}; t)}(\mathbf{y}) d\sigma_d(\mathbf{z}) dt \\ &= \int_{-1}^1 \int_{\mathbb{S}^d} g_1(\mathbf{z}, t) \mathbf{1}_{C(\mathbf{z}; t)}(\mathbf{y}) d\sigma_d(\mathbf{z}) dt \\ &= f_1(\mathbf{y}), \end{aligned}$$

showing that the inner product (11.4) has the reproducing property. By [Aronszajn \(1950\)](#), the inner product in $\mathcal{H}_{v, h, \mathbf{x}'}$ is unique. Functions f_i satisfying (11.3) with $\langle f_i, f_i \rangle_{K_{v, h, \mathbf{x}'}} < \infty$ are in $\mathcal{H}_{v, h, \mathbf{x}'}$, and (11.4) is the unique inner product of $\mathcal{H}_{v, h, \mathbf{x}'}$.

We prove the theorem by equating two different forms of $\|\mathcal{R}(\mathcal{H}_{v, h, \mathbf{x}'}; \cdot)\|_{K_{v, h, \mathbf{x}'}}$ where

$$\mathcal{R}(\mathcal{H}_{v, h, \mathbf{x}'}; \cdot) = \int_{\mathbb{S}^d} K_{v, h, \mathbf{x}'}(\cdot, \mathbf{y}) d\sigma_d(\mathbf{y}) - \frac{1}{N} \sum_{k=0}^{N-1} K_{v, h, \mathbf{x}'}(\cdot, \mathbf{x}_k).$$

Although $\mathcal{R}(\mathcal{H}_{v, h, \mathbf{x}'}; \cdot)$ depends on our specific points \mathbf{x}_i we omit that from the notation. The reproducing property of $K_{v, h, \mathbf{x}'}$ yields

$$\langle K_{v, h, \mathbf{x}'}(\cdot, \mathbf{x}_k), K_{v, h, \mathbf{x}'}(\cdot, \mathbf{x}_\ell) \rangle_{K_{v, h, \mathbf{x}'}} = K_{v, h, \mathbf{x}'}(\mathbf{x}_k, \mathbf{x}_\ell)$$

from which it follows that

$$\begin{aligned} &\left\langle \int_{\mathbb{S}^d} K_{v, h, \mathbf{x}'}(\cdot, \mathbf{y}) d\sigma_d(\mathbf{y}), \int_{\mathbb{S}^d} K_{v, h, \mathbf{x}'}(\cdot, \mathbf{y}') d\sigma_d(\mathbf{y}') \right\rangle_{K_{v, h, \mathbf{x}'}} \\ &= \int_{\mathbb{S}^d} \int_{\mathbb{S}^d} K_{v, h, \mathbf{x}'}(\mathbf{y}, \mathbf{y}') d\sigma_d(\mathbf{y}) d\sigma_d(\mathbf{y}'). \end{aligned} \quad (11.5)$$

Using (11.5) and the linearity of the inner product, we have

$$\begin{aligned}
& \langle \mathcal{R}(\mathcal{H}_{v,h,\mathbf{x}'; \cdot}), \mathcal{R}(\mathcal{H}_{v,h,\mathbf{x}'; \cdot}) \rangle_{K_{v,h,\mathbf{x}'}} \\
&= \int_{\mathbb{S}^d} \int_{\mathbb{S}^d} K_{v,h,\mathbf{x}'}(\mathbf{y}, \mathbf{y}') d\sigma_d(\mathbf{y}) d\sigma_d(\mathbf{y}') - \frac{2}{N} \sum_{k=0}^{N-1} \int_{\mathbb{S}^d} K_{v,h,\mathbf{x}'}(\mathbf{y}, \mathbf{x}_k) d\sigma_d(\mathbf{y}) \\
&+ \frac{1}{N^2} \sum_{k,\ell=0}^{N-1} K_{v,h,\mathbf{x}'}(\mathbf{x}_k, \mathbf{x}_\ell).
\end{aligned} \tag{11.6}$$

For our second form of $\|\mathcal{R}(\mathcal{H}_{v,h,\mathbf{x}'; \cdot})\|_{K_{v,h,\mathbf{x}'}}$, we write

$$\begin{aligned}
& \mathcal{R}(\mathcal{H}_{v,h,\mathbf{x}'; \cdot}) \\
&= \int_{\mathbb{S}^d} K_{v,h,\mathbf{x}'}(\cdot, \mathbf{y}) d\sigma_d(\mathbf{y}) - \frac{1}{N} \sum_{k=0}^{N-1} K_{v,h,\mathbf{x}'}(\cdot, \mathbf{x}_k) \\
&= \int_{-1}^1 v(t) \int_{\mathbb{S}^d} \mathbf{1}_{C(\mathbf{z};t)}(\mathbf{x}) h(\langle \mathbf{z}, \mathbf{x} \rangle) \left[\int_{\mathbb{S}^d} \mathbf{1}_{C(\mathbf{z};t)}(\mathbf{y}) d\sigma_d(\mathbf{y}) dt - \frac{1}{N} \sum_{k=0}^{N-1} \mathbf{1}_{C(\mathbf{z};t)}(\mathbf{x}_k) \right] d\sigma_d(\mathbf{z}) dt \\
&= \int_{-1}^1 v(t) \int_{\mathbb{S}^d} \mathbf{1}_{C(\mathbf{z};t)}(\mathbf{x}) h(\langle \mathbf{z}, \mathbf{x} \rangle) \left[\sigma_d(C(\mathbf{z}, t)) - \frac{1}{N} \sum_{k=0}^{N-1} \mathbf{1}_{C(\mathbf{z};t)}(\mathbf{x}_k) \right] d\sigma_d(\mathbf{z}) dt.
\end{aligned}$$

Hence using the definition of the inner product $\langle \cdot, \cdot \rangle_{K_{v,h,\mathbf{x}'}}$, we have

$$\begin{aligned}
& \langle \mathcal{R}(\mathcal{H}_{v,h,\mathbf{x}'; \mathbf{x}}), \mathcal{R}(\mathcal{H}_{v,h,\mathbf{x}'; \mathbf{x}}) \rangle_{K_{v,h,\mathbf{x}'}} \\
&= \int_{-1}^1 v(t) \int_{\mathbb{S}^d} h(\langle \mathbf{z}, \mathbf{x} \rangle) \left| \sigma_d(C(\mathbf{x}, t)) - \frac{1}{N} \sum_{k=0}^{N-1} \mathbf{1}_{C(\mathbf{x};t)}(\mathbf{x}_k) \right|^2 d\sigma_d(\mathbf{x}) dt.
\end{aligned} \tag{11.7}$$

Combining equations (11.6) and (11.7), we have the generalized location-weighted version of the Stolarsky invariance principle. \square

11.5. Proof of Theorem 8 (Spatially weighed invariance)

As in Section 11.1, $\lim_{\epsilon \rightarrow 0}$ means $\lim_{\epsilon_1 \rightarrow 0^+} \lim_{\epsilon_2 \rightarrow 0^+}$ and similarly $\lim_{\eta \rightarrow 0}$ denotes $\lim_{\eta_1 \rightarrow 0^+} \lim_{\eta_2 \rightarrow 0^+}$. We prove a series of lemmas first.

Lemma 7. For $v_\epsilon(\cdot)$ and $h_\eta(\cdot)$ defined by equations (3.3) and (5.3),

$$\begin{aligned}
& \lim_{\eta \rightarrow 0} \lim_{\epsilon \rightarrow 0} \int_{-1}^1 v_\epsilon(t) \int_{\mathbb{S}^d} h_\eta(\langle \mathbf{z}, \mathbf{x}_c \rangle) \left| \sigma_d(C(\mathbf{z}, t)) - \frac{1}{N} \sum_{k=0}^{N-1} \mathbf{1}_{C(\mathbf{z};t)}(\mathbf{x}_k) \right|^2 d\sigma_d(\mathbf{z}) dt \\
&= \int_{\mathbb{S}^{d-1}} |p(\tilde{\rho} \mathbf{x}_c + \sqrt{1 - \tilde{\rho}^2} \mathbf{y}^*, \hat{\rho}) - \hat{p}_1(\hat{\rho})|^2 d\sigma_{d-1}(\mathbf{y}^*),
\end{aligned}$$

where $\hat{p}_1(\hat{\rho}) = \sigma_d(C(\mathbf{y}; \hat{\rho}))$.

Proof. This proof is similar to the others. First we take the limit $\epsilon \rightarrow 0$ yielding

$$\lim_{\eta \rightarrow 0} \int_{\mathbb{S}^d} h_\eta(\langle \mathbf{z}, \mathbf{x}_c \rangle) \left| \sigma_d(C(\mathbf{z}, \hat{\rho})) - \frac{1}{N} \sum_{k=1}^N \mathbf{1}_{C(\mathbf{z}; \hat{\rho})}(\mathbf{x}_k) \right|^2 d\sigma_d(\mathbf{z}).$$

Making the projection $\mathbf{z} = s\mathbf{x}_c + \sqrt{1-s^2}\mathbf{z}^*$ gives

$$\begin{aligned} & \lim_{\eta \rightarrow 0} \int_{-1}^1 \int_{\mathbb{S}^{d-1}} \frac{\omega_{d-1}}{\omega_d} (1-s^2)^{d/2-1} h_\eta(s) \times \\ & \quad \left| \sigma_d(C(s\mathbf{x}_c + \sqrt{1-s^2}\mathbf{z}^*, \hat{\rho})) - \frac{1}{N} \sum_{k=1}^N \mathbf{1}_{C(s\mathbf{x}_c + \sqrt{1-s^2}\mathbf{z}^*; \hat{\rho})}(\mathbf{x}_k) \right|^2 d\sigma_{d-1}(\mathbf{z}^*) ds \\ & = \int_{\mathbb{S}^{d-1}} |p(\hat{\rho}\mathbf{x}_c + \sqrt{1-\hat{\rho}^2}\mathbf{y}^*, \hat{\rho}) - \hat{p}_1(\hat{\rho})|^2 d\sigma_{d-1}(\mathbf{y}^*). \quad \square \end{aligned}$$

Lemma 8. For $v_\epsilon(\cdot)$ and $h_\eta(\cdot)$ defined by equations (3.3) and (5.3),

$$\begin{aligned} & \lim_{\eta \rightarrow 0} \lim_{\epsilon \rightarrow 0} \frac{1}{N^2} \sum_{k, \ell=0}^{N-1} K_{v_\epsilon, h_\eta, \mathbf{x}_c}(\mathbf{x}_k, \mathbf{x}_\ell) \\ & = \frac{1}{N^2} \sum_{k, \ell=0}^{N-1} \int_{\mathbb{S}^{d-1}} \mathbf{1}(\langle \mathbf{y}, \mathbf{x}_k \rangle \geq \hat{\rho}) \mathbf{1}(\langle \mathbf{y}, \mathbf{x}_\ell \rangle \geq \hat{\rho}) d\sigma_{d-1}(\mathbf{y}^*). \end{aligned}$$

Proof. First, $\lim_{\eta \rightarrow 0} \lim_{\epsilon \rightarrow 0} N^{-2} \sum_{k, \ell=0}^{N-1} K_{v_\epsilon, h_\eta, \mathbf{x}_c}(\mathbf{x}_k, \mathbf{x}_\ell)$ equals

$$\frac{1}{N^2} \sum_{k, \ell=0}^{N-1} \lim_{\eta \rightarrow 0} \int_{\mathbb{S}^d} h_\eta(\langle \mathbf{z}, \mathbf{x}_c \rangle) \mathbf{1}_{C(\mathbf{z}; \hat{\rho})}(\mathbf{x}_k) \mathbf{1}_{C(\mathbf{z}; \hat{\rho})}(\mathbf{x}_\ell) d\sigma_d(\mathbf{z}).$$

Projecting \mathbf{z} onto \mathbf{x}_c yields $\mathbf{z} = s\mathbf{x}_c + \sqrt{1-s^2}\mathbf{y}^*$ and then we have

$$\begin{aligned} & \frac{1}{N^2} \sum_{k, \ell=0}^{N-1} \lim_{\eta \rightarrow 0} \int_{-1}^1 \frac{\omega_{d-1}}{\omega_d} (1-s^2)^{d/2-1} h_\eta(s) \int_{\mathbb{S}^{d-1}} \mathbf{1}_{C(\mathbf{z}; \hat{\rho})}(\mathbf{x}_k) \mathbf{1}_{C(\mathbf{z}; \hat{\rho})}(\mathbf{x}_\ell) d\sigma_{d-1}(\mathbf{y}^*) \\ & = \frac{1}{N^2} \sum_{k, \ell=0}^{N-1} \int_{\mathbb{S}^{d-1}} \mathbf{1}(\langle \mathbf{y}, \mathbf{x}_k \rangle \geq \hat{\rho}) \mathbf{1}(\langle \mathbf{y}, \mathbf{x}_\ell \rangle \geq \hat{\rho}) d\sigma_{d-1}(\mathbf{y}^*). \quad \square \end{aligned}$$

Lemma 9. For $v_\epsilon(\cdot)$ and $h_\eta(\cdot)$ defined by equations (3.3) and (5.3),

$$\lim_{\eta \rightarrow 0} \lim_{\epsilon \rightarrow 0} \int_{\mathbb{S}^d} \int_{\mathbb{S}^d} K_{v_\epsilon, h_\eta, \mathbf{x}_c}(\mathbf{x}, \mathbf{y}) d\sigma_d(\mathbf{x}) d\sigma_d(\mathbf{y}) = \hat{p}_1(\hat{\rho})^2$$

Proof. Because $K_{v_\epsilon, h_\eta, \mathbf{x}_c}$ is nonnegative and uniformly bounded we may take the limit over ϵ inside the integrals. Now

$$\lim_{\epsilon \rightarrow 0} K_{v_\epsilon, h_\eta, \mathbf{x}_c}(\mathbf{x}, \mathbf{y}) = \int_{\mathbb{S}^d} h_\eta(\langle \mathbf{z}, \mathbf{x}_c \rangle) \mathbf{1}_{C(\mathbf{z}; \hat{\rho})}(\mathbf{x}) \mathbf{1}_{C(\mathbf{z}; \hat{\rho})}(\mathbf{y}) d\sigma_d(\mathbf{z}),$$

and the limit becomes

$$\lim_{\eta \rightarrow 0} \int_{\mathbb{S}^d} \int_{\mathbb{S}^d} \int_{\mathbb{S}^d} h_\eta(\langle \mathbf{z}, \mathbf{x}_c \rangle) \mathbf{1}_{C(\mathbf{z}; \hat{\rho})}(\mathbf{x}) \mathbf{1}_{C(\mathbf{z}; \hat{\rho})}(\mathbf{y}) \, d\sigma_d(\mathbf{z}) \, d\sigma_d(\mathbf{x}) \, d\sigma_d(\mathbf{y}).$$

Integrating over \mathbf{z} last we get $\lim_{\eta \rightarrow 0} \int_{\mathbb{S}^d} h_\eta(\langle \mathbf{z}, \mathbf{x}_c \rangle) \hat{p}_1^2(\hat{\rho}) \, d\mathbf{z} = \hat{p}_1^2(\hat{\rho})$. \square

Lemma 10. *Under reference distribution 2*

$$\lim_{\eta \rightarrow 0} \lim_{\epsilon \rightarrow 0} \frac{2}{N} \sum_{k=0}^{N-1} \int_{\mathbb{S}^d} K_{v_\epsilon, h_\eta, \mathbf{x}_c}(\mathbf{x}, \mathbf{x}_k) \, d\sigma_d(\mathbf{x}) = 2\hat{p}_1(\hat{\rho}) \mathbb{E}(p(\mathbf{y}, \hat{\rho})).$$

Proof. The argument here is similar to the one used for Lemma 9. Take the limit over ϵ inside the integral and change the order of integration to yield

$$\lim_{\eta \rightarrow 0} 2\hat{p}_1(\hat{\rho}) \int_{\mathbb{S}^d} \frac{1}{N} \sum_{k=0}^{N-1} h_\eta(\langle \mathbf{z}, \mathbf{x}_c \rangle) \mathbf{1}_{C(\mathbf{z}, \hat{\rho})}(\mathbf{x}_k) \, d\sigma_d(\mathbf{z}).$$

Substituting the projection $\mathbf{z} = t\mathbf{x}_c + \sqrt{1-t^2}\mathbf{z}^*$ produces

$$\begin{aligned} & \lim_{\eta \rightarrow 0} 2\hat{p}_1(\hat{\rho}) \int_{-1}^1 \frac{\omega_{d-1}}{\omega_d} (1-t^2)^{d/2-1} h_\eta(t) \int_{\mathbb{S}^{d-1}} \frac{1}{N} \sum_{k=0}^{N-1} \mathbf{1}_{C(t\mathbf{x}_c + \sqrt{1-t^2}\mathbf{z}^*, \hat{\rho})}(\mathbf{x}_k) \, d\sigma_{d-1}(\mathbf{z}^*) \, dt \\ &= 2\hat{p}_1(\hat{\rho}) \int_{\mathbb{S}^{d-1}} \frac{1}{N} \sum_{k=0}^{N-1} \mathbf{1}_{C(\hat{\rho}\mathbf{x}_c + \sqrt{1-\hat{\rho}^2}\mathbf{z}^*, \hat{\rho})}(\mathbf{x}_k) \, d\sigma_{d-1}(\mathbf{z}^*) \\ &= 2\hat{p}_1(\hat{\rho}) \mathbb{E}(p(\mathbf{y}, \hat{\rho})) \end{aligned}$$

for \mathbf{y} under Model 2. \square

Proof of Theorem 8

Proof. The proof follows from using Lemmas 7 to 10 and Theorem 7. \square